POWER QUALITY IMPROVEMENT BASED ON HYBRID DIFFERENTIAL EVOLUTION OPTIMIZATION AND ARTIFICIAL NEURAL NETWORKS USING BATTERY ENERGY STORAGE

BY

JABER ALI ALSHEHRI

A Thesis Presented to the
DEANSHIP OF GRADUATE STUDIES

KING FAHD UNIVERSITY OF PETROLEUM & MINERALS

DHAHRAN, SAUDI ARABIA

In Partial Fulfillment of the
Requirements for the Degree of

MASTER OF SCIENCE

In

ELECTRICAL ENGINEERING

DECEMBER 2019

KING FAHD UNIVERSITY OF PETROLEUM & MINERALS

DHAHRAN- 31261, SAUDI ARABIA

DEANSHIP OF GRADUATE STUDIES

This thesis, written by **JABER ALI ALSHEHRI** under the direction of his thesis advisor and approved by his thesis committee, has been presented and accepted by the Dean of Graduate Studies, in partial fulfillment of the requirements for the degree of **MASTER OF SCIENCE IN ELECTRICAL ENGINEERING**.

Dr. Muhammad Khalid
(Advisor)

Dr. Abdullah S. Al-Ahmari
Department Chairman

Dr. Ibrahim El-Amin
(Member)

Dr. Salam A. Zummo
Dean of Graduate Studies

عمادة الدراسات العليا
DEANSHIP OF GRADUATE STUDIES

Dr. Fahad S. Al-Ismail
(Member)

31/12/19
Date

Dedicated to

My Beloved Parents

And

My Brothers and Sisters

ACKNOWLEDGMENTS

First and foremost, all praises and thanks are for ALLAH SWT alone, who provided me with the required knowledge to successfully complete my MSc degree in electrical engineering at King Fahd University of Petroleum & Minerals (KFUPM). Peace and blessings be upon the greatest man ever, the last and the final Prophet, Muhammad (peace be upon him), upon his family, his companions, and all those who follow him until the day of judgment. I am extremely thankful to my thesis advisor Dr. Muhammad Khalid for his invaluable guidance throughout this research. I always admired his knowledge and inspiration, which successfully instilled in me a passion for scientific research. I would also like to thank him for his friendship, empathy, and great dedication. It was a true honor to work and study under his supervision. Many thanks go to my committee members Dr. Ibrahim El-Amin and Dr. Fahad Al-Ismail, for their valuable feedback and time that they spent in this thesis. I would like to express my deepest gratitude, appreciation, and thanks to my beloved parents for their love, prayers, and sacrifices that they have made to educate and prepare me for my future. Words cannot explain the feelings I have for them. I would also like to thank all my brothers and sisters for always standing by my side in hard and soft times. I owe a deep appreciation to my manager Eng. Hussain Bin Mashni at the protection engineering division - NG, for his persistent support and cooperation during my study. A very special thanks to my wonderful colleagues, Ahmed Alzahrani and Hussain Alharthi, for being always very supportive and helpful. It was really my pleasure and honor that we have made it together through this study journey over the past three years. Last but not the least, I acknowledge KFUPM for providing all the required essential learning tools and facilities to complete my research.

TABLE OF CONTENTS

LIST OF TABLES

LIST OF FIGURES

LIST OF ABBREVIATIONS

A. ABBREVIATIONS

ANN	:	Artificial neural networks
BESS	:	Battery energy storage system
DEO	:	Differential evolution optimization
DER	:	Distrusted energy resources
DESS	:	Distributed energy storage system
DG	:	Distrusted generation
DGS	:	Distrusted generation system
DSG	:	Diesel synchronous generator
D-axis	:	Direct axis
EA	:	Evolutionary algorithms
EP	:	Evolutionary programming
ES	:	Evolution strategy
ESD	:	Energy storage devices
ESS	:	Energy storage system
FC	:	Fuel cells

FESS	:	Flywheel energy storage system
FL	:	Fuzzy logic
FR	:	Frequency restoration
GA	:	Genetic algorithm
GEL	:	Gelified electrolyte batteries
GP	:	Genetic programming
GT	:	Gas turbines
HIL	:	Hardware-in-loop
HT	:	Hydropower turbines
IAE	:	Integral of absolute error
ICE	:	Internal combustion engines
IGBT	:	Insulated-gate bipolar transistor
ISE	:	Integral squared error
ITAE	:	Integral of time multiplied absolute error
ITSE	:	Integral of time multiplied squared error
LA	:	Lead-acid batteries
LI	:	Lithium-ion batteries

LM	:	Levenberg-Marquardt
LP	:	Low-pass
MG	:	Microgrid
MLFFNN	:	Multi-layer feed-forward neural network
MSE	:	Mean-squared error
OV	:	Overshoot
PCC	:	Point of common coupling
PI	:	Proportional-integral
PID	:	Proportional-integral-derivative
PSO	:	Particle swarm optimization
PV	:	Photovoltaic system
PWM	:	Pulse-width modulation
Q-axis	:	Quadrature axis
RES	:	Renewable energy sources
RPS	:	Reactive power sharing
SCESS	:	Super-capacitor energy storage system
SG	:	Synchronous generator

SLD	:	Single line diagram
SMES	:	Superconducting magnetic energy storage
ST	:	Settling time
VSC	:	Voltage source converter
VSI	:	Voltage source inverter
WT	:	Wind turbine
ZN	:	Ziegler-Nichols

B. PARAMETERS

ω_0	:	Reference angular frequency
H	:	Inertia constant
T_{d0}'	:	Open circuit field constant
x_d	:	D-axis synchronous reactance
x'_d	:	D-axis transient reactance
τ_E	:	Exciter time constant
α_E	:	Exciter gain
V_{g0}	:	SG reference terminal voltage

E_{fd0}	:	Reference field voltage in d-axis
L_b	:	Boost converter inductor
d_{pv}	:	Boost converter duty ratio
C_{dcpv}	:	DC linking capacitor
R_{pf}	:	LP Filter resistance
L_{pf}	:	LP Filter inductance
R_{pdr}	:	Damping resistor
R_p	:	Transmission line coupling resistance
L_p	:	Transmission line coupling inductance
C_{pf}	:	LP Filter capacitor
R_B	:	Battery storage resistance
C_{dcs}	:	DC linking capacitance
R_{st}	:	Resistance of VSC
L_{st}	:	Inductance of VSC
V_0	:	Reference PCC bus voltage

C. VARIABLES

δ	:	Angular displacement
ω	:	Angular frequency
E_{fd}	:	Field voltage in d-axis
e_q'	:	Internal voltage in q-axis
P_e	:	Output electrical power
P_m	:	Input mechanical power
i_{PV}	:	PV cell output current
V_{dcpv}	:	PV DC linking capacitor voltage
i_{pfd}	:	VSI output current in d-axis
i_{pfq}	:	VSI output current in q-axis
m_{PV}	:	PV inverter modulation index
ψ_{PV}	:	PV inverter phase angle
V_{cpd}	:	LP filter capacitor voltage in d-axis
V_{cpq}	:	LP filter capacitor voltage in q-axis

i_{pd}	:	LP filter output current in d-axis
i_{pq}	:	LP filter output current in q-axis
V_{dcs}	:	Battery DC linking capacitor voltage
i_{std}	:	BESS output current in d-axis
i_{stq}	:	BESS output current in q-axis
m_B	:	Battery-VSC modulation index
ψ_B	:	Battery-VSC phase angle
K_P	:	Controller proportional gain
K_I	:	Controller integral gain
K_D	:	Controller derivative gain
$K_{P\omega}$	:	Frequency controller proportional gain
$K_{I\omega}$	:	Frequency controller integral gain
K_{Pv}	:	Voltage controller proportional gain
K_{Iv}	:	Voltage controller integral gain

ABSTRACT

Full Name : [JABER ALI ALSHEHRI]

Thesis Title : [Power Quality Improvement Based on Hybrid Differential Evolution Optimization and Artificial Neural Networks Using Battery Energy Storage]

Major Field : [Electrical Engineering]

Date of Degree : [December 2019]

Modern power systems rely on renewable energy sources (RESs) and distributed generation systems (DGSs) more than ever before; the combination of those two, along with the advanced energy storage systems, contributed widely to the development of microgrids (MGs). MGs provide flexibility to integrate renewables into the power network. Nevertheless, the transience of most RESs exacerbates the power quality of the grid network. Furthermore, the unpredictability of RESs additionally becomes challenging in the case of unknown disturbances. The deployment and optimal utilization of energy storage systems, to act as an energy buffer are hence pertinent. One of the significant technical challenges in MG applications is to improve the power quality of the system subjected to unknown disturbances; particularly, the problem sometimes becomes very challenging in case of unknown disturbances with significantly higher magnitude. Hence intelligent control approaches are vital to cope with the problem.

In this work, two innovative online intelligent control approaches based on battery energy storage system (BESS) are proposed to improve the power quality of a MG system. The objective is the restoration of system voltage and frequency considering a wide range of disturbances and hence circumvent the power quality degradation. To the best of

author’s knowledge, the proposed approaches in this thesis have not been proposed earlier in the literature. The first proposal utilizes a single BESS-based controller, whereas, the second proposal utilizes two decoupled BESS-based controllers. The MG system under consideration in this research consists of two distributed generators, a diesel synchronous generator, and a photovoltaic power system, integrated with a BESS. The detailed nonlinear equations that represent the dynamic model of the MG system are provided.

The two designed control approaches are based on a hybrid differential evolution optimization (DEO) and artificial neural network (ANNs) technique. The controller parameters have been optimized under several operating conditions using the DEO. The obtained input and output patterns are consequently used to train the ANNs in order to perform an online tuning for the controller parameters. Finally, the effectiveness of the two proposed control approaches has been validated under random low and high level disturbances as compared with a benchmark controller. The simulation results show the effectiveness of the first proposal at low level disturbances, as well as prove the robustness of the second proposed control approach at low and high level disturbances

ملخص الرسالة

الاسم الكامل: جابر بن علي الشهري

عنوان الرسالة: تحسين جودة الطاقة بطريقة التطور التفاضلي وشبكات الخلايا العصبية باستخدام أنظمة تخزين الطاقة

التخصص: هندسة كهربائية

تاريخ الدرجة العلمية: ديسمبر 2019

أصبحت الشبكات الكهربائية الحديثة تعتمد على مصادر الطاقة المتجددة وتقنيات تخزين الطاقة بشكل غير مسبوق، مما أسهم في انتشار وتطور الشبكات الكهربائية لتصبح شبكات ذكية. تسهل الشبكات الكهربائية الذكية من إمكانية ربط مصادر الطاقة المتجددة بشبكة الكهرباء. ولكن مع ربط هذه المصادر الحديثة للطاقة ظهرت تحديات جديدة تؤثر بدورها على عمل واستقرار الشبكات الكهربائية. أحد أهم هذه التحديات هو تأثير ربط مصادر الطاقة المتجددة على أداء واستقرار الشبكة خصوصا في حال حدوث اضطرابات كبيرة للشبكة. لذلك هناك حاجة ماسة لتقنيات تحكم ذكية تدعم وتعزز من استقرار الشبكة. هذه الرسالة تقدم مقترح لتقنيتي تحكم ذكيتين للمحافظة على استقرار الشبكة وتحسين جودة الطاقة الكهربائية وذلك باستخدام بطاريات تخزين الطاقة. الهدف الأساسي من تطبيق تقنيات التحكم الذكية هو المحافظة على استقرار الجهد الكهربائي والتردد في حال حدوث اضطرابات مفاجأة للشبكة. على حد علم المؤلف فإن تقنيات التحكم الذكية المقترحة في هذه الأطروحة لم يسبق أبداً اقتراحها مسبقاً من قبل أخرين. المقترح الأول في هذه الرسالة هو استخدام جهاز تحكم ذكي واحد لتحسين جودة الطاقة والمقترح الثاني هو باستخدام جهازي تحكم ذكيين للتحكم بالبطاريات بالشبكة الكهربائية الذكية. تمت برمجت أجهزة التحكم بطريقة التطور التفاضلي وشبكات الخلايا العصبية الاصطناعية. وقد تم اختبار طرق التحكم المبتكرة في هذه الأطروحة وأثبتت النتائج فعاليتها في تحسين جودة الطاقة والمحافظة على أداء واستقرار الشبكة الكهربائية.

CHAPTER 1

INTRODUCTION

1.1 Background

The limited resources for conventional power generation, in combination with environmental concern, has brought about the need for integrating renewable energy resources (RESs) into the existing power grid, such as photovoltaics (PVs), wind turbines (WTs) and hydropower turbines (HTs) [1]. The consolidation of RESs has significantly changed the structural topology of conventional power networks from centralized power generation to distributed generation (DG); typically, small-scale power generations that lie in the close proximity to the load centers [2].

The power quality and reliability of conventional radial distribution networks in several countries have degraded. As per [3], the definition of power quality is "the capability of the electricity grid to provide customers reliable, ideal and non-tolerant electricity". Power quality issues in power systems include outages, voltage dips, overvoltage, under-voltage, voltage swell, transients, frequency oscillation, noise distortion, and harmonics. In accordance, the concept of MG is adopted to obviate and circumvent these power quality deficiencies [4], [5]. Small-scale power generation systems (PV, WT, etc.), loads, and energy storage devices (ESDs) are typically the general attributes of MG [6]-[8]. MGs can be operated on either grid-connected mode or islanded mode [9]. The control requirements vary based on the operating mode and the controlled components such as DGs, ESDs, and loads [10]. The small-scale DGs can be categorized on the basis of their grid interface as, inertial type or inverter type. Hence, DGs like gas turbines (GTs), micro alternators and, internal combustion engines (ICEs) are classified as inertial-type DGs that can be directly integrated into the conventional AC grid. Accordingly, the inverter-type DGs require a power electronic interface for grid connection and consists of a power generation system such as PV, WT, and fuel cells (FCs) [11]-[15].

The ESDs constitute as an energy buffer and contribute to various aspects of power quality improvement [16]. In this front, numerous energy storage systems (ESSs) have been employed, such as flywheel energy storage systems (FESSs), super-capacitor energy storage systems (SCESSs), superconducting magnetic energy storage systems (SMESs) and battery energy storage systems (BESSs) [17]-[19]. A comprehensive review of ESS technologies, classifications, configurations, features, characteristics, advantages, and disadvantages in MG applications is presented in [20].

In addition to the integration of environmentally friendly power generation sources, RES-MGs offer lower financial responsibilities as compared to conventional centralized bulk power generation. Furthermore, the sensitivity of load towards transmission line interruptions is less severe. In short, valuable goals can be achieved, such as decrement in carbon emissions as well as lower investment costs and enhanced reliability of power supply [21], [22]. Nevertheless, the implementation of MGs has many regulatory and technical challenges. The technical challenges imposed consist of power quality degradation, coordination of protective relays, and dynamic stability issues [23]. Whereas, regulated government pricing, uncompetitive electricity market, and convenient geographical locations for RESs are the associated regulatory challenges [24], [25].

Recently, the concept of MGs has substantially gained global interest. Many kinds of academic and industrial research have been conducted to propose and implement various kinds of MG systems and their associated control strategies for deployment alongside conventional power networks. For instance, the MG project of China [26], the MG project of Venezuela [27], the MG project in Barcelona (Spain) [28], the MG research in Federal University of Rio de Janeiro in Brazil [29], and several projects in the United States [30].

1.2 Thesis Motivation

MG systems experience disturbances due to many reasons. These disturbances include a sudden loss of power generation, short circuits, and sudden load changes [31], [32]. Therefore, a proper control strategy is highly needed to improve the power quality and restore the system to its initial steady-state condition in case of contingencies.

The main theme of this thesis is to study the behavior of the MG system under various unknown levels of disturbances. Accordingly, two intelligent control approaches have been proposed to improve the MG power quality by restoring the system frequency and voltage to steady-state conditions. The MG system under consideration in this thesis works on grid-connected mode and consists of two distributed generations, which are diesel synchronous generator (DSG) and PV power system. In order to improve the system power quality during transients, two intelligent BESS-based control approaches are proposed. The BESS is interfaced through voltage source converter (VSC) to provide an additional active and reactive power support for the MG system. The controller parameters will be optimized under several levels of disturbances using differential evolution optimization (DEO) technique. These disturbances simulate sudden changes in the input mechanical torque of the DSG. The optimized controller parameters and the corresponding disturbances are arranged in input and output patterns for training the artificial neural network (ANN). Finally, the two proposed control approaches have been evaluated under random disturbances, and their performance has been compared with a benchmark proportional-integral-derivative (PID) controller.

1.3 Thesis Objectives

The main theme of this thesis is to study the dynamic behavior of the grid-connected MG system under various unknown levels of disturbances. Accordingly, two BESS-based intelligent control approaches based on hybrid differential evolution optimization and artificial neural network (DEO-ANN) are proposed to improve the MG power quality. In particular, frequency and voltage restoration to steady-state conditions are targeted.

The thesis objectives are listed as follows:

1. A comprehensive literature review on various power quality improvement techniques in microgrid systems.

2. Mathematical modeling of a battery-generator-PV coupled microgrid system.

3. Design of a standalone intelligent controller to improve the microgrid power quality subjected to low level disturbances.

4. Proposing a two-controller based configuration of a microgrid system to enhance power quality subjected to critical disturbances.

5. A comparative study of a single controller and multiple controllers to handle low and high levels disturbances.

1.4 Thesis Outcomes

Number of journal and conference publications are the outcomes of the thesis, as follows.

1. J. Alshehri and M. Khalid, "Power Quality Improvement in Microgrids Under Critical Disturbances Using an Intelligent Decoupled Control Strategy Based on Battery Energy Storage System," in *IEEE Access*, vol. 7, pp. 147314-147326, 2019.

2. J. Alshehri, M. Khalid and A. Alzahrani, "An Intelligent Battery Energy Storage-Based Controller for Power Quality Improvement in Microgrids", in *Energies*, vol. 12, no. 11, pp. 2112, Jun. 2019.

3. J. Alshehri, A. Alzahrani and M. Khalid "Voltage and Frequency Control of Microgrids with Distributed Generations and Battery Energy Storage", *in the proceedings of the 2019 International Conference on Renewable Energy Research and Applications (ICRERA)*, Brasov, Romania, 2019.

4. J. Alshehri, A. Alzahrani, M. Khalid and F. Alismail "Optimal Control Strategy for Battery Energy Storage Systems Based on Hybrid Differential Evolution and Neural Networks", *in the proceedings of the 2020 IEEE PES Transmission & Distribution (T&D) Conference*, Chicago, IL, USA.

1.5 Thesis Organization

This thesis is organized in 6 chapters. The contents of these chapters are described in the following:

- Chapter 1 introduces the work in the thesis by giving a brief background of microgrids' advantages and challenges. After that, the thesis motivation, objectives, and organization are presented.
- Chapter 2 provides a brief literature review about the microgrid and its components, the control architectures, and the resent power quality improvement techniques.
- Chapter 3 describes in detail the mathematical modeling and the circuit models of each component of the microgrid system under consideration in this thesis.
- Chapter 4 presents the two proposed approaches in this thesis for power quality improvement in microgrids, which are a single BESS-based controller and double BESS-based controllers.
- Chapter 5 discusses in detail the simulation results for the two proposed approaches and evaluate the performance of the proposals as compared with a benchmark controller.
- Chapter 6 concludes the work in this thesis by highlighting the most important findings as well as proposes future research work.

CHAPTER 2

LITERATURE REVIEW

This chapter provides a summary of the recent researches performed on electrical MGs. In this thesis, the literature review is divided into three sections. The first section provides an overview of MGs definition and categories. In addition, it describes the benefits of MGs, the implementation challenges, and the basic components of a MG system. The second section summarized some of the MG control architectures and approaches proposed in the literature. The third and last section focuses on the latest power quality improvement techniques that can be employed in MG applications.

2.1 Microgrid Definition and Categories

The basic idea of electrical microgrid systems refers to a small scale of the power system that consists of distributed generators, energy storage devices, and loads operating together as one system [33]. Initially, MGs introduced to manage generators in smaller quantities rather than managing a huge network; however, nowadays, a modern and small-scale version of a centralized utility is highly needed [34]. Electrical microgrid systems can be categorized into four classes. The first one is remote grids, which are essential because of geographical landscapes, for instance, islands. The next class is the military grids, where the highest security is strongly needed in order to keep data and security throughout a national disaster. The third class is commercial or industrial grids that supply a particular industrial or commercial community and finally, community grids [35].

Using microgrid brings in several advantages such as lower financial responsibility compared to bulk power generation, utilizing renewable resources, no effect as of grid interruption, and minimizing the sum of consumers' dependence on network generating capacity. In short, the main goals, such as reliability, lower carbon emission, and cost-saving, are achieved. MGs can work on on-grid mode or islanded operation mode. The operation and control requirements vary based on the operating mode [36]. For instance, operating in an islanded mode requires energy storage to enhance system stability [37].

MGs consist of DGs, which refer to a small scale of power generation units that are placed close to or at load site. Nowadays, DGs modern technologies provide plants with high efficiency and ranging in nominal capacity from a few kW to hundreds of MW [38], [39]. The high cost of constructing long transmission lines can be reduced by placing the DGs near or at the load centers. One of the major types of DGs is renewable energy sources RES that significantly contribute to reducing greenhouse emissions [40]. Nonetheless, RESs are built with the help of using modern power electronics that increase the system dependability as well as the quality of the power supply [41], [42]. The energy storage devices are mandatory to balance energy when a system disturbance occurred. Furthermore, renewable energy sources such as Photovoltaic panels are weather dependents. Hence, ESD is necessary to overcome such unbalanced conditions. The ESDs can be seen as controllable AC voltage sources that perform actions when the system suddenly affected by any unbalanced conditions [43].

One of the essential components of MGs nowadays is energy storage. The need for energy storage solutions has been required since the early stages of the electrical power system, for example, storing energy for later use or provide assistance to system operators to mitigate stability issues in power networks. However, with the recently growing number of RES deployment in power systems, the energy storage systems become vital. Since RES categorized as weather dependent, there is a need to harvest the available energy to supply demand and store the surpluses energy for later use. Further, energy storage devices can be used for several applications; for example, it can be used as an AC voltage source that can be fully controlled to assist the power system in responding to sudden effects caused by abnormal disturbances [44]. The allocation of energy storage systems can be categorized as aggregated, semi-distributed, and distributed topology. For example, in MG applications, it is possible to have a centralized energy storage option or decentralized energy storage dedicated for each DGs [45]. The most common energy storage systems are super-capacitors and traditional batteries. Super-capacitors provide high energy charge/discharge rate, hence short response time, but they are expensive as compared with batteries. Whereas, the traditional batteries are less expensive, but they provide large power, which is desirable in most applications such as microgrids [46].

The increasing deployment of microgrids that contain non-inertial electronically coupled DG sources has posed many technical operational issues [47]. These issues include harmonics generation, uncertainty, and intermittency of the renewable DGs, power quality degradation, and active and reactive power sharing among the DGs in the MG system. The harmonics generated by the electronic switching, e.g., boost converters or DC/AC inverters, can be mitigated by proper design and installation of harmonics filters. Whereas, the uncertainty and intermittency of the weather-dependent renewable DGs sources can be overcome by optimal allocation, sizing, and control of energy storage devices in grid-connected or off-grid microgrid systems [48].

2.2 Microgrid Control Architectures

The arrangement of MGs stipulates the control requirements. Usually, the control of MGs is subjected to the type of elements that need to be controlled. For example, to control a specific load, the parameters of real power, reactive power, and voltage are targeted. In accordance with the literature, MGs' control strategies are broadly categorized into centralized and decentralized control architecture [49], as shown in Figure 2.1.

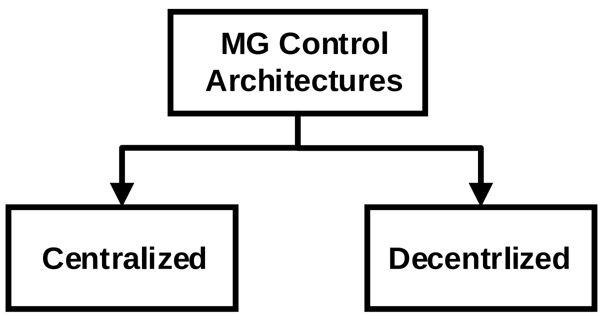

Figure 2.1. MG control architectures.

In centralized control, the entire system is handled by a central control unit that shares data and information with a distribution control system through communication channels [50]. In this regard, centralized MG control is presented in [51]. Here, the control strategy is based on the particle swarm optimization (PSO) and fuzzy logic (FL) technique for tuning the parameters of the proportional-integral (PI). The PI parametric tuning is carried according to the online measurements using FL rules. The membership functions of the FL are optimized using PSO. The authors postulated better frequency regulation (FR) in comparison to classical PI controllers and pure fuzzy-based PI controllers.

The authors in [52] have presented a centralized MG controller to provide a communication channel with the distribution system operator and the electricity market as well as to exchange information with the MG local controllers. Similarly, in [53], the authors have proposed a centralized controller for energy management in an isolated MG system that works in islanded operation mode. In [54], the authors have presented a centralized control strategy for optimal power sharing and voltage regulations for a set of inverter-based DGs in a MG system. The proposed method has been tested and proved its effectiveness. In [55], the authors have proposed a centralized control strategy DRG and ESS coordination in an autonomous MG system. The proposed control approach aimed to coordinate the operation of the renewable DGs as well as the energy storage devices in order to have a reliable operation of the islanded MG system. The role of ESS was to regulate the amplitude of the MG bus voltage and stabilize the MG system frequency. The authors have experimentally verified the performance of their proposed centralized controller in a lab-scale MG system.

In decentralized control, a dedicated controller is designed for each component of the MG system [56]. A decentralized control approach for FR and reactive power sharing (RPS) is demonstrated in [57]. In this research, power-frequency droop control is designed where the line voltage drop compensation is used to generate the frequency reference and to improve the voltage droop coefficient. Furthermore, a voltage feedback control is introduced to achieve an accurate RPS. The control strategy proposed in this study proves to flexibly and effectively operate under various DG disturbance scenarios. Similarly, a decentralized control strategy directed towards the bidirectional power converter interface that is implemented for optimal AC/DC MG integration has been studied in [58]. The main objective of the proposed control method is to achieve overall power-sharing and smooth transition between grid-connected and autonomous mode. Moreover, an ESS is utilized in the DC sub-grid to provide voltage support during the islanded mode operation. The authors verified the performance of this control strategy by real-time hardware-in-loop (HIL) tests. In [59], a decentralized control approach of a microgrid system for stability enhancement is proposed. The proposed control approach utilized a wireless network to exchange information about the active and reactive power of the MG's DGs. The proposed strategy aimed to achieve optimal power sharing based on a droop control strategy.

In [60], the authors have developed a decentralized power control approach to control and manage the active power in an AC single-phase MG system. The proposed control approach enables the MG system inverter to operate smoothly in both on-grid and off-grid operation modes. Similarly, a decentralized control technique is proposed in [61] to control the DGs and loads on the MG system using the MG frequency variations. The proposed strategy aimed to achieve optimal power flow among the MG system components. The authors in [62] have proposed a coordinated control architecture to manage the power in an AC autonomous MG with RESs and ESSs. The authors have derived a smooth switching droop control to achieve optimal decentralized power management in the MG system. Their proposal has been tested, and several scenarios have been simulated by the real-time HIL in order to validate the effectiveness of the proposed control strategy.

Accordingly, other centralized and decentralized control strategies have been proposed in [63]-[73] for optimal operation of MG systems in both grid-connected and islanded operation modes.

2.3 Power Quality Improvement in Microgrids

Energy storage systems are widely used to enhance the power quality and provide stability support to MG systems in both grid-connected as well as islanded mode [74], [75]. Moreover, energy storage can be implemented in a low inertia power system to provide virtual inertia and enhance system stability during abnormalities [76]. Numerous prospective ESS-based control strategies have been studied in the literature.

The authors in [77] have proposed a BESS to support the system frequency and improve the power quality of a MG system subjected to high penetration of RESs. Moreover, a conventional droop control method, along with a virtual inertia function is utilized to enhance the MG system stability. The simulation and experimental results prove the effectiveness of the proposed approach in grid-connected and islanded MGs. A control strategy for energy storage to mitigate the impact of PV and wind in isolated low inertia systems is proposed in [78]. The authors have utilized an ultra-capacitors besides distributed energy storage systems (DESSs) to perform a dynamic frequency control support for an islanded French power system. The results claim that the use of fast-acting ultra-capacitors and DESSs can mitigate the negative impact of non-inertia renewable generations during major system outages.

In [79], a power management control strategy in AC islanded MG system is proposed. The authors have considered a MG system that consists of DESSs and PV generation to feed local loads. The proposed control approach can efficiently regulate the active power-sharing on the MG and hence, achieving maximum utilization of the RESs and the DESSs. In order to validate the performance of the proposed power regulation strategy, a real-time simulation under different scenarios has been performed by the authors. The authors in [80] have proposed an efficient control technique for power quality enhancement and voltage profile improvement at the PCC bus in a MG system. The proposed controller performs optimal power management by a single-phase converter connected to the MG phases arbitrarily. The controller works based on the Master/Slave principle, where the distributed slave controllers are controlled by a central master controller. The proposed control approach has been tested in simulation based on real data of a distribution network.

The authors in [81] have presented a novel power sharing control algorithm based on droop control in an AC MG system that consists of both inertial and non-inertial DGs. The main objective was to improve the MG power quality by compensating the non-linear loads of the MG system and achieve optimal power-sharing among the DGs of the MG. In [82], a PI controller, a proportional-resonant, and dead beat controllers have been proposed for power quality improvement in MG systems. However, the proposed technique is applicable only for balanced MG systems. The authors in [83] have proposed a control strategy based on hierarchical control theory for active power quality improvement in a grid-connected MG system. The unbalanced voltage at the PCC bus and the harmonics generated by the inverter-based DGs have degraded the power quality of the MG system. Hence, the authors have proposed the aforementioned control approach to circumvent power quality degradation. The simulation and experimental results on a lab-scale MG system have been presented in order to verify and prove the effectiveness of their proposal.

In [84], a PID-fuzzy controller for BESS is proposed to enhance the power quality in MGs. The efficient utilization of ESS for power quality improvement and, consequently, the overall performance of the system are enhanced further as compared with classical PI controllers. Further, the study in [85], proposes a controller for BESS that has been designed for voltage and frequency restoration during MG system transience. The designed controller has been explicitly tested for two abnormal conditions of the MG; abrupt load changes and fault conditions. However, the performance of these two BESS-based controllers was not satisfactory in terms of response time and fluctuations magnitude. The study in [86], proposes a BESS-based control strategy to enhance the power quality in grid-tied MGs. However, this strategy is suitable only for low-level disturbances.

Likewise, in [87], a SCESS-based controller for MG frequency support is proposed. The controller approach based on structural singular value theory and using the DEO technique to optimize the SCESS controller gains corresponding to the MG requirements. This methodology effectively supports the MG frequency to compensate for system transience conditions. However, it does not improve the MG system voltage, as well. In [88], a control strategy to support and regulate the frequency and voltage of the MG during system contingencies have been proposed considering a hybrid energy storage system (HESS), which consists of BESS and SCESS along with DGs such as PV, WT, FC, and micro-generators. The author has employed a PI-based adaptive online neuro-fuzzy algorithm for optimal power allocation between the HESS components.

Accordingly, other techniques have been proposed in [89]-[99] to achieve rapid dynamic response under abnormal conditions of the MG. However, these proposed techniques do not contribute significantly towards improving the power quality and additionally involve complex and tedious calculations.

CHAPTER 3

MICROGRID SYSTEM MODEL

3.1 Introduction

This chapter describes in detail the dynamic model of the components of the MG system. The MG system model is decomposed into three sections. The mathematical nonlinear differential equations for the diesel synchronous generator is given the first section. The second section presents the model of the PV system along with the boost converter, voltage source inverter, and the low pass filter. Finally, the last section demonstrates the mathematical modeling of the battery energy storage system.

The MG under consideration has two DG sources integrated and connected to the PCC bus. In addition, the BESS interfaced through a VSC along with the static loads and connected to the MG. Figure 3.1 shows the single line diagram (SLD) of the MG system.

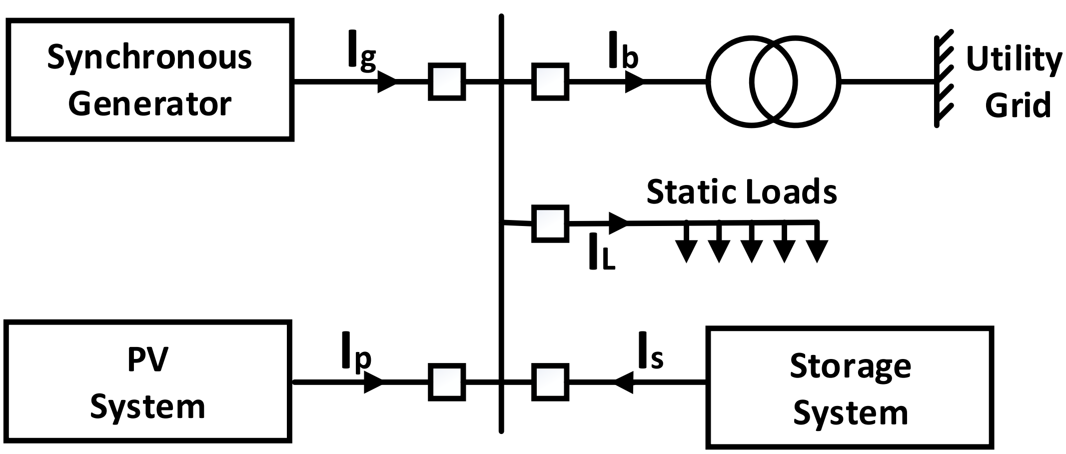

Figure 3.1. The single line diagram MG system.

The MG system can be modeled by several mathematical nonlinear differential equations that represent its dynamic behavior. Figure 3.2 shows the detailed layout of the MG system under investigation in this work.

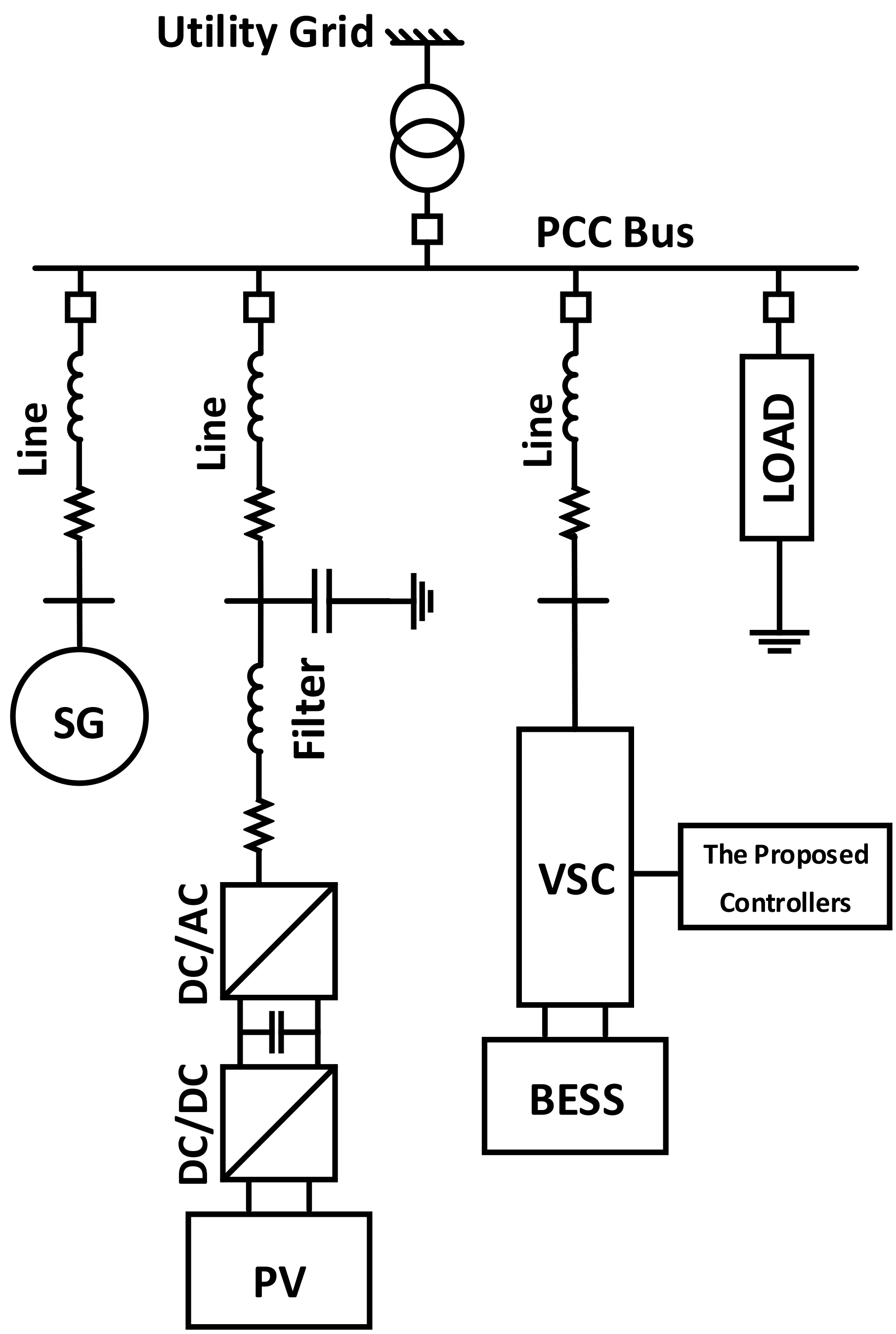

Figure 3.2. The detailed layout of the MG system.

The following sections provide detailed mathematical representations of each component of the MG system under consideration in this work.

3.2 Diesel Synchronous Generator

The DSG can be modeled by four nonlinear first-order differential equations [86]. Two equations represent the mechanical part of the generator and decomposed from the well-known swing equation. The angular displacement of the generator rotor δ and angular speed ω are mathematically described as:

$$\frac{d\delta}{dt} = \omega_0 \left(\omega - 1 \right) \tag{3.1}$$

$$\frac{d\omega}{dt} = \frac{1}{2H} \left(P_m - P_e \right) \tag{3.2}$$

Where ω_0, H, P_e, and P_m are the reference angular frequency, the inertia constant, the output electrical power, and the input mechanical power.

The other two equations represent the electrical part of the generator. The expression in (3.3) describes the field voltage along the direct axis (d-axis) of the generator's rotor E_{fd}. While the expression in (3.4) describes the internal voltage along the quadrature axis (q-axis) of the generator's rotor e_q', as follows:

$$\frac{dE_{fd}}{dt} = \frac{1}{\tau_E} \left[\alpha_E \left(V_{g0} - V_g \right) - \left(E_{fd} - E_{fd0} \right) \right] \tag{3.3}$$

$$\frac{de_q'}{dt} = \frac{1}{T_{d0}'} \left[E_{fd} - e'_e - \left(x_d - x'_d \right) i_{gd} \right] \tag{3.4}$$

Where T_{d0}', x_d, x'_d, τ_E, α_E, V_{g0}, and E_{fd0} are the open circuit field constant, the d-axis synchronous reactance, the d-axis transient reactance, the exciter time constant, the exciter gain, the SG reference voltage, and the d-axis reference field voltage, respectively. The state variables of the DSG model are given as:

$$X_{DSG} = [\delta, \omega, E_{fd}, e_q']$$

3.3 Solar Photovoltaic System

The solar cell is the fundamental block of the PV system, and it consists mainly of a current source, diode, and resistance. In the literature, there are many equivalent circuit models for the solar photovoltaic system. The equivalent circuit shown in Figure 3.3 is called the Simplified-PV model, which consists of a current source, a diode, and a resistor.

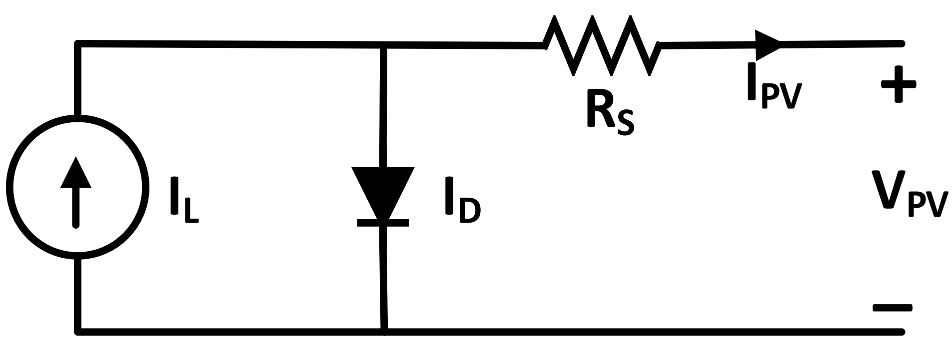

Figure 3.3. PV cell simplified circuit model.

The PV system can be modeled mathematically by eight nonlinear first-order differential equations [86]. These equations represent the dynamic behavior of the PV cell, the DC/DC boost converter, the D/AC voltage source inverter, the low-pass (LP) filter, and the coupling transmission line as well.

3.3.1 The DC/DC Boost Converter

The equivalent circuit of the DC/DC boost converter is shown in Figure 3.4. It consists of an energy-storing inductor, an insulated-gate bipolar transistor (IGBT) switch, a forward acting diode, and a DC-Link capacitor to filter the DC boost converter voltage and maintain constant input voltage to the DC/AC inverter.

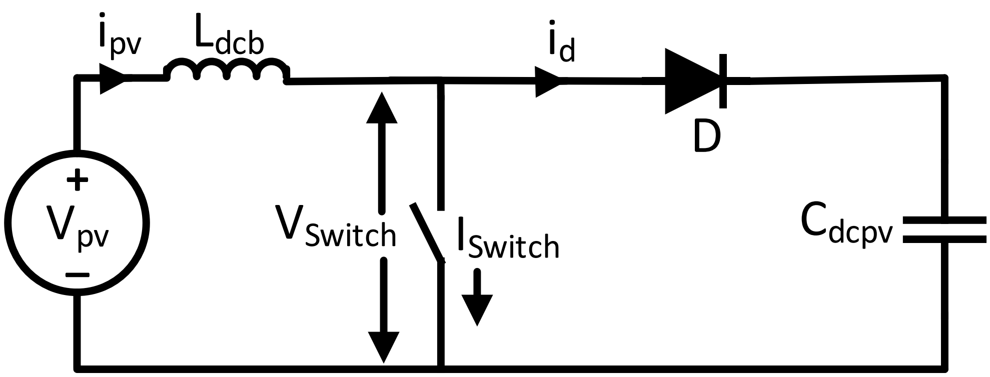

Figure 3.4. The Boost converter circuit.

The relations (3.5) and (3.6) represent the PV output current i_{PV} and the DC link output voltage after the DC/DC converter V_{dcpv}, respectively.

$$\frac{di_{pv}}{dt} = \frac{1}{L_b}\left[V_{pv} - \left(1 - d_{pv}\right)V_{dcpv}\right] \tag{3.5}$$

$$\frac{dv_{dcpv}}{dt} = \frac{1}{C_{dcpv}}\left[\left(1 - d_{pv}\right)i_{pv} - m_{pv} i_{pfd} \cos\left(\psi_{pv} + \theta\right)\right] \tag{3.6}$$

Where L_b, d_{pv}, C_{dcpv}, m_{PV}, and ψ_{PV} are the boost converter inductor, the boost converter duty ratio, the DC linking capacitor, the PV inverter modulation index, and the PV inverter phase angle, respectively.

3.3.2 The DC/AC Voltage Source Inverter

The voltage source DC/AC inverter (VSI) operated in pulse-width modulation (PWM) mode with a modulation index m_{pv} and a phase angle ψ_{pv}. The inverter is essential to convert the DC power to an AC in order to integrate the PV system with the PCC bus. Figure 3.5 shows the DC/AC inverter circuit model.

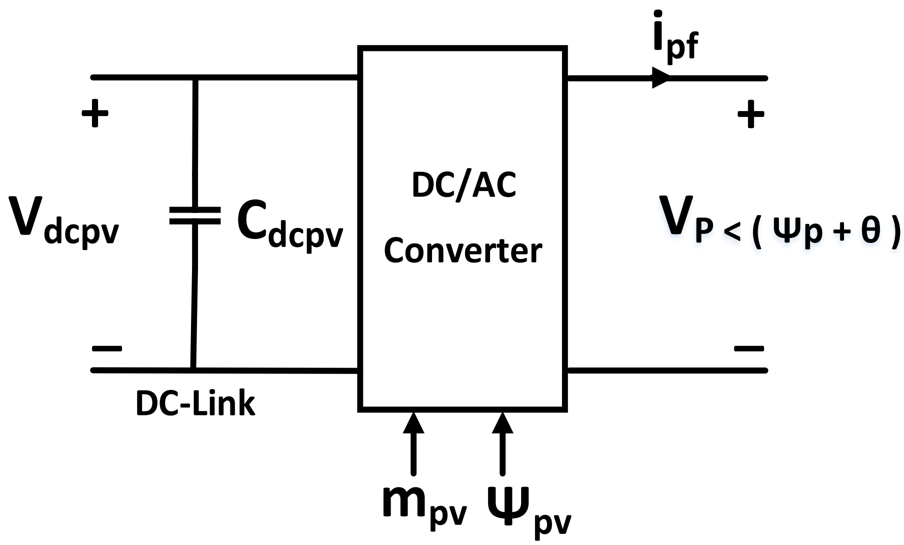

Figure 3.5. The voltage source inverter circuit model.

The mathematical expressions in (3.7) and (3.8) represent the inverter output current in d-axis i_{pfd}, the inverter output current in q-axis i_{pfq}, respectively.

$$\frac{di_{pfd}}{dt} = \frac{-\omega_0 R_{pf}}{L_{pf}} i_{pfd} + \omega_0 \omega i_{pfq} + \frac{\omega_0 m_{pv} V_{dcpv} \cos\left(\psi_{pv} + \theta\right)}{L_{pf}} - \frac{\omega_0 V_{cpd}}{L_{pf}} - \omega_0 R_{pdr}\left(i_{pfd} - i_{pd}\right) \quad (3.7)$$

$$\frac{di_{pdq}}{dt} = \frac{-\omega_0 R_{pf}}{L_{pf}} i_{pfq} + \omega_0 \omega i_{pfd} + \frac{\omega_0 m_{pv} V_{dcpv} \sin\left(\psi_{pv} + \theta\right)}{L_{pf}} - \frac{\omega_0 V_{cpq}}{L_{pf}} - \omega_0 R_{pdr}\left(i_{pfq} - i_{pq}\right) \quad (3.8)$$

Where R_{pf}, L_{pf}, and R_{pdr} are the LP filter resistance, the LP filter inductance, and the damping resistor, respectively.

3.3.3 The Low Pass Filter

The low pass (LP) filter circuit and the coupling transmission line model are shown in Figure 3.6. It consists of parallel and series resistance, inductance, and capacitance. The LP filter is essential to mitigate the harmonics from the AC system.

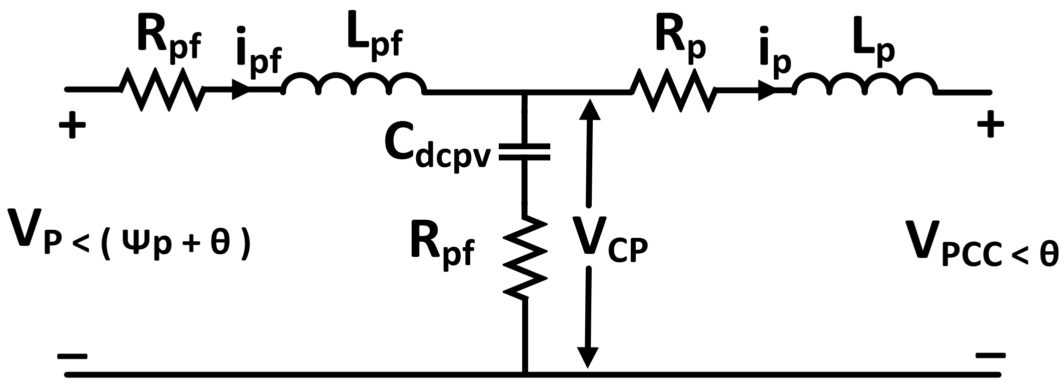

Figure 3.6. The LP filter and transmission line model.

The LP filter capacitor voltage in d-axis V_{cpd}, the LP filter capacitor voltage in q-axis V_{cpq}, the LP filter output current in d-axis i_{pd}, and the LP filter output current in q-axis i_{pq} are expressed in the expressions (3.9), (3.10), (3.11) and (3.12), respectively.

$$\frac{dV_{cpd}}{dt} = \frac{1}{C_{pf}}\left(i_{pfd} - i_{pd}\right) + \omega_0 \omega V_{cpq} \tag{3.9}$$

$$\frac{dV_{cpq}}{dt} = \frac{1}{C_{pf}}\left(i_{pfq} - i_{pq}\right) + \omega_0 \omega V_{cpd} \tag{3.10}$$

$$\frac{di_{pd}}{dt} = \frac{-\omega_0 R_p}{L_p} i_{pd} + \omega_0 \omega i_{pq} + \frac{\omega_0}{L_p}\left(V_{cpd} - V_{sd}\right) + \omega_0 R_{pdr}\left(i_{pfd} - i_{pd}\right) \tag{3.11}$$

$$\frac{di_{pq}}{dt} = \frac{-\omega_0 R_p}{L_p} i_{pq} + \omega_0 \omega i_{pd} + \frac{\omega_0}{L_p}\left(V_{cpq} - V_{sq}\right) + \omega_0 R_{pdr}\left(i_{pfq} - i_{pq}\right) \tag{3.12}$$

Where R_p, L_p, and C_{pf} are the Transmission line coupling resistance, Transmission line coupling inductance, and the LP Filter capacitor, respectively.

The state variables of the PV system model are given as:

$$X_{PV} = [i_{pv}, V_{dcpv}, i_{pfd}, i_{pfq}, V_{cpd}, V_{cpq,} i_{pd}, i_{pq}]$$

3.4 Battery Energy Storage System

The BESS can be modeled as a single DC source connected in series with a resistor and integrated with the PCC bus through a VSC, as shown in Figure 3.7. The expressions given in (3.13), (3.14), and (3.15) represents the DC-link capacitor voltage V_{dcs}, the BESS output current in d-axis i_{std}, and the BESS output current in q-axis i_{stq}, respectively [86].

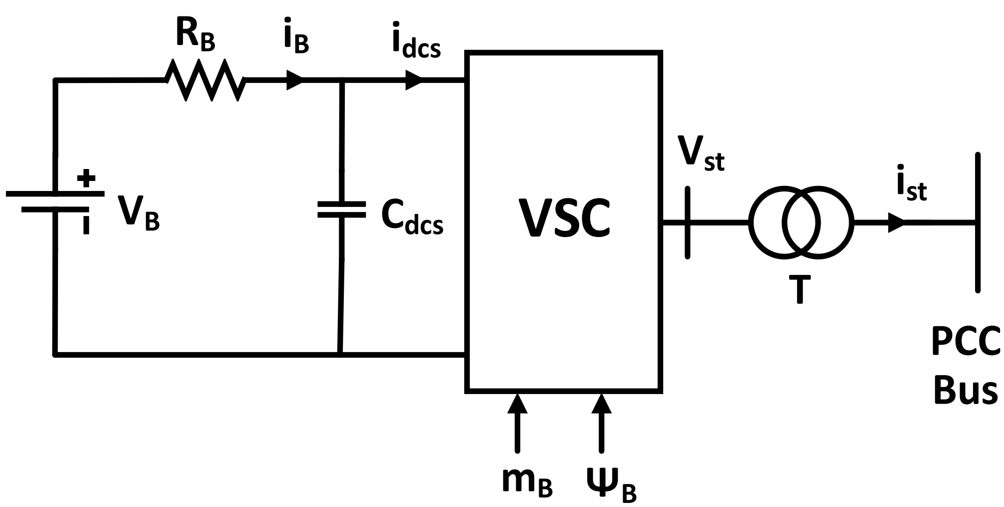

Figure 3.7. The **BESS** circuit model.

$$\frac{dV_{dcs}}{dt} = \frac{m_B}{C_{dcs}}(i_{stq}\cos(\psi_B) + i_{stq}\sin(\psi_B)) + \frac{V_B - V_{dcs}}{R_B C_{dcs}} \tag{3.13}$$

$$\frac{di_{std}}{dt} = \frac{-\omega_0 R_{st}}{L_{st}} i_{std} + \frac{\omega}{\omega_0} i_{stq} + \frac{\omega_0}{L_{st}}(m_B V_{dcs}\cos(\theta + \psi_B) - V_{sd}) \tag{3.14}$$

$$\frac{di_{stq}}{dt} = \frac{-\omega_0 R_{st}}{L_{st}} i_{stq} + \frac{\omega}{\omega_0} i_{std} + \frac{\omega_0}{L_{st}}(m_B V_{dcs}\sin(\theta + \psi_B) - V_{sq}) \tag{3.15}$$

Where m_B and ψ_B are the battery-VSC modulation index and phase angle, respectively.

The state variables of the BESS model are given as:

$$X_{BESS} = [i_{std}, i_{stq}, V_{dcs}]$$

So the total state variables of the whole MG system model are 15 variables as follows:

$$X_{MG} = [\delta, \omega, E_{fd}, e_q', i_{pv}, V_{dcpv}, i_{pfd}, i_{pfq}, V_{cpd}, V_{cpq}, i_{pd}, i_{pq}, i_{std}, i_{stq}, V_{dcs}]$$

CHAPTER 4

THE PROPOSED APPROACH

This chapter minutely illustrates the two proposed intelligent control approaches in this thesis for power quality improvement in the MG system. It is divided into two sections. The first section explains the single BESS-based control approach which is applicable only for low-level disturbances. Whereas, the second section describes the double BESS-based control approach which is robust for low and critical disturbances.

4.1 Single BESS-Based Controller

4.1.1 Problem Formulation

The aim is to improve the MG power quality by restoring the system frequency and voltage to the steady-state condition in case of having a disturbance in the input mechanical power of the DSG. To solve this optimization problem, the optimal design of the PI controller that gives the minimum frequency error shall be carried out. Therefore, the objective function is to minimize the system frequency integral squared-error (ISE) as follows:

$$Min\int_0^t (\Delta\omega)^2 dt = \int_0^t (\omega_0 - \omega)^2 dt \tag{4.1}$$

In doing so, some constraints on the PI controller limits shall be met. The Kp and Ki parameters shall be as follows:

$$70 \leq \mathrm{Kp} \leq 250$$

$$70 \leq \mathrm{Ki} \leq 250$$

The acceptable operating limits of the MG frequency and voltage are given in Table 4.1.

Table 4.1. MG acceptable operating limits.

Quantity	**Minimum value (p.u)**	**Maximum value (p.u)**
Frequency	0.999	1.001
voltage	0.95	1.05

The predefined ranges for the controller parameters are required to ensure that the response of the system will not violate the prescribed operation limits for the MG frequency and voltage. The limits for the controllers' parameters have been determined by trial and error during the simulation and observing the optimal parameter values that do not adversely jeopardize the response of the system.

4.1.2 The Proposed Control Methodology

The proposed control methodology in this work is to use hybrid DEO and ANN techniques to optimize the BESS-based PI controller. The main role of the energy storage-based PI controller is to improve the power quality and restore the system to its steady-state condition after the occurrence of a disturbance. In order to achieve this type of control, a proper selection of the controller parameters is required. Figure 4.1 shows the control block diagram of the MG system, where the system frequency is compared to a reference frequency. The mismatch between the two frequencies represents the error that needs to be minimized. Then, this error signal is entered into the PI controller, and the output control signal will be as per (4.2). The DEO-ANN algorithm will generate the optimal controller parameters (Kp & Ki) depending on the disturbance level.

$$Control\_Signal = K_P \times e(t) + K_i \times \int_0^t e(t)dt \tag{4.2}$$

The control signal will control the VSC of the BESS through the modulation index (m) and the phase angle (ψ). Accordingly, the BESS will supply or absorb both active (P) and reactive power (Q) depending on the system needs. The real power will enhance the dynamic performance through quick damping of the oscillations. Consequently, the MG frequency returns to the steady-state condition. While the reactive power will improve the voltage recovery at the PCC bus. As a result, the MG power quality is improved.

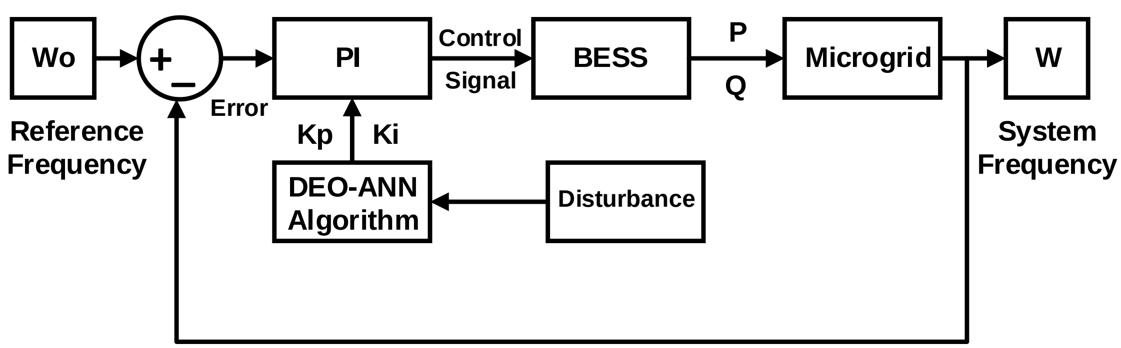

Figure 4.1. MG control diagram model.

The DEO algorithm is being used as an optimization technique to find the optimal values of the controller gains. The DEO is one type of the evolutionary algorithms (EAs) which are population-based optimization techniques. Other EAs include genetic algorithms

(GA), genetic programming (GP), evolutionary programming (EP), and evolution strategy (ES) [100]. The DEO is distinguished by its simplicity, robustness and fast convergence. Also, DEO is suitable to solve systems that can be represented by non-linear differential equations [101]. Since the MG system under consideration consists of several non-linear differential equations, the DEO technique is proposed in this work to optimize the parameters of the PI controller. The parameter settings of the DEO algorithm are shown in Table 4.2. The optimal generation number and population size are determined by experience and by trial and error during the simulation until the best performance is achieved. Whereas, typical values are chosen for the crossover and mutation factors.

Table 4.2. The DEO parameter settings.

Parameter description	Value
Generation number	50
Population size	20
Crossover factor	0.5
Mutation factor	0.5

The flow chart of the proposed methodology is shown in Figure 4.2. The algorithm starts with the initialization of DEO, and then different levels of disturbances applied to the input mechanical torque of DSG. These disturbances simulate sudden changes in the mechanical part of the DSG. Both the optimum solutions (Kp and Ki) and the disturbance level for each operating condition are obtained and stored. Then, these stored parameters are used to train the ANN. Once the ANN is trained, then the weighting matrices can identify the parameters for a particular operating condition within the training range.

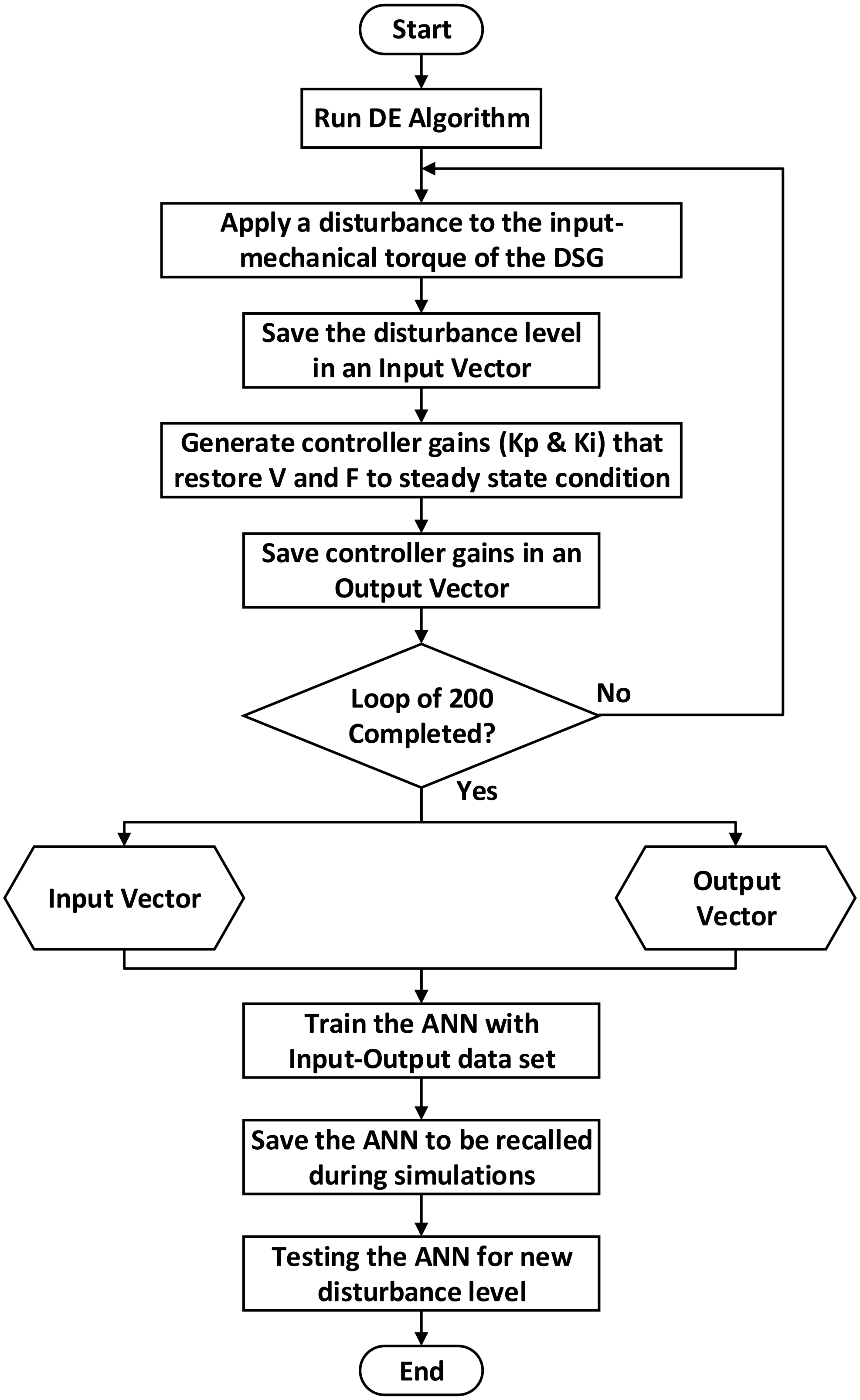

Figure 4.2. Flowchart of the proposed approach.

Figure 4.3 shows the developed ANN model. As can be observed, it consists of an input layer with 200 levels of disturbances ranging from 0.2 p.u to 0.8 p.u, a hidden layer with 200 neurons, and an output layer with two neurons that give the optimized controller parameters Kp and Ki. The backpropagation algorithm has been used as a training algorithm with a hyperbolic tangent activation function for the hidden neurons and a linear activation function for the output neurons.

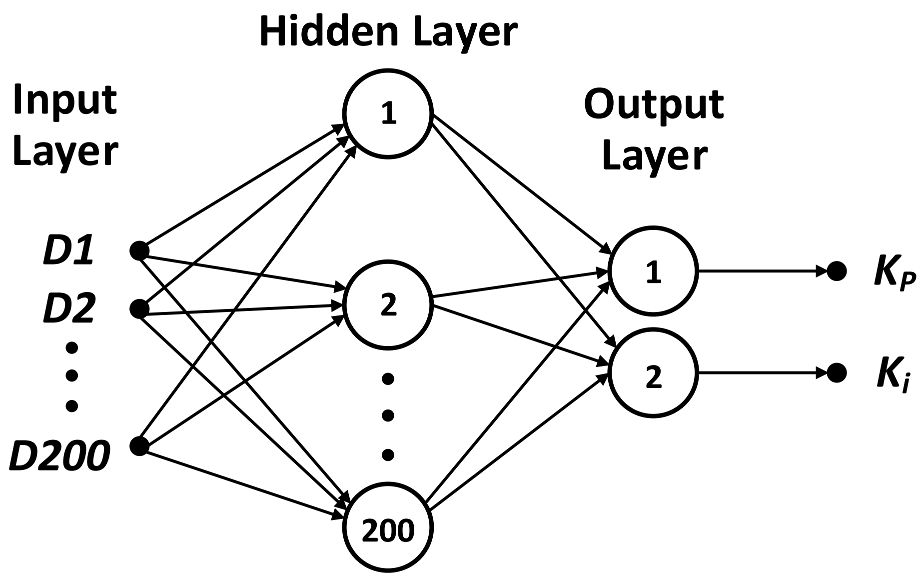

Figure 4.3. The ANN model.

Figure 4.4 shows the performance curve of the developed ANN that has been trained to give the optimal PI controller parameters for any disturbance within the training range. It can be observed clearly that the best training performance found to be at Epoch number **4** with mean-squared error (MSE) converges to zero, which indicates that the developed ANN is very well trained.

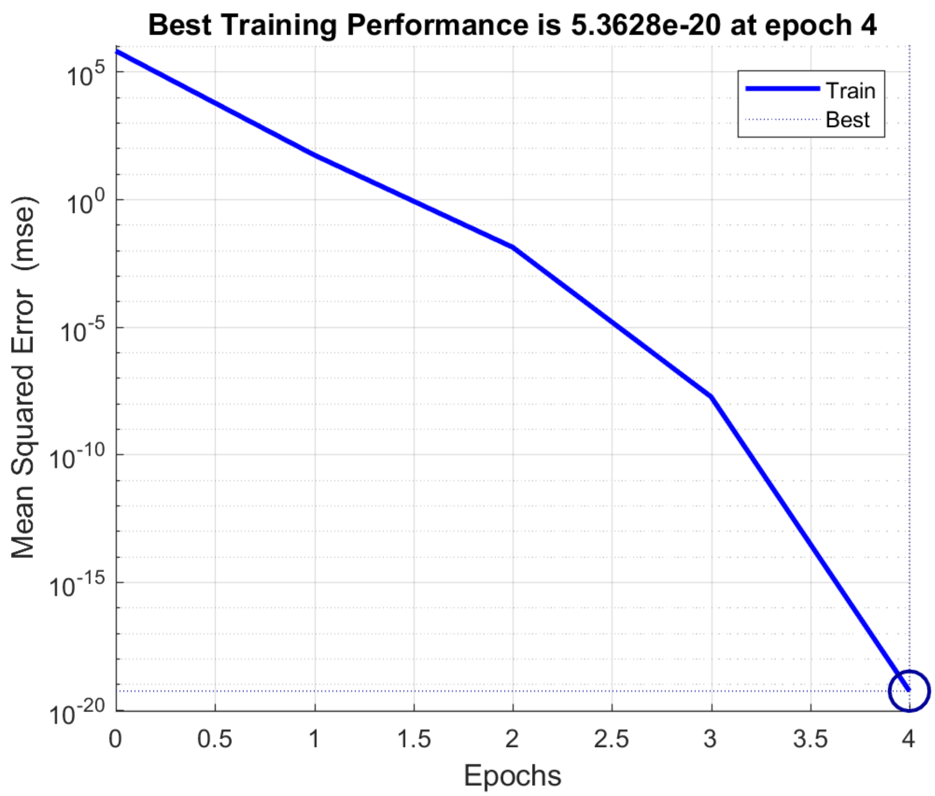

Figure 4.4. The ANN training performance curve.

4.2 Double BESS-Based Controllers

4.2.1 Problem Formulation

In this section, two intelligent decoupled BESS-based PI controllers are proposed to improve the MG power quality by restoring the MG voltage and frequency to normal operating conditions following a disturbance. The two intelligent controllers are designed based on hybrid DEO and ANN techniques. The MG voltage and frequency are decoupled by independently controlling the BESS output active and reactive power.

Figure 4.5 shows the proposed control approach diagram, where the phase angle and the modulation index of the VSC are controlled separately by two BESS-based PI controllers. The phase angle controls the BESS active power needed to be supplied or absorbed. Whereas, the modulation index controls the amount of reactive power required to be supplied or absorbed by the BESS. As per the expressions (4.3) and (4.4), the voltage and frequency of the MG are compared with reference values at first. Then, the mismatches, which represent errors, are entered into the two PI controllers in order to be minimized. After that, the developed hybrid approach tunes the controllers with the optimal parameters based on the disturbance level.

$$m_B = K_{Pv} e_v(t) + K_{Iv} \int_0^t e_v(t) dt \tag{4.3}$$

$$\psi_B = K_{P\omega} e_\omega(t) + K_{I\omega} \int_0^t e_\omega(t) dt \tag{4.4}$$

Consequently, the BESS supplies or absorbs the needed amount of active and reactive power, based on the stability requirements of the MG system. The active power will enhance MG frequency by damping the system oscillations. Whereas, the reactive power will improve the MG PCC bus voltage profile. As a result, the overall power quality of the MG system is improved.

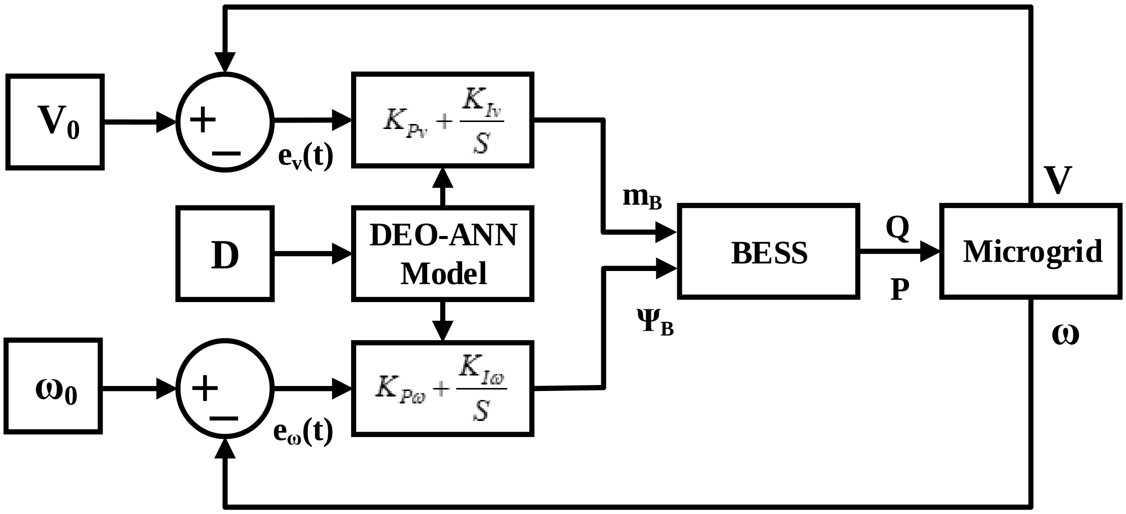

Figure 4.5. The proposed control approach diagram.

Searching the optimal controllers' parameters can be formulated as two optimization problems, where the two objective functions are the minimization of the voltage ISE (4.5) and the frequency ISE (4.6).

$$Min\int_0^t e_v(t)^2 dt = \int_0^t (\Delta V)^2 dt = \int_0^t (V_0 - V)^2 dt \tag{4.5}$$

$$Min\int_0^t e_\omega(t)^2 dt = \int_0^t (\Delta \omega)^2 dt = \int_0^t (\omega_0 - \omega)^2 dt \tag{4.6}$$

The two objective functions are subjected to the following constraints:

- The permissive operation limits of MG frequency and PCC bus voltage in per-unit (p.u.) values.

$$0.999 \le Frequency \le 1.001$$

$$0.95 \le Voltage \le 1.05$$

- The two PI controllers' parameters limits and maximum overshoot response.

$$30 \le K_{P\omega}, K_{Pv} \le 150$$

$$50 \le K_{I\omega}, K_{Iv} \le 250$$

$$Overshoot \le 10\%$$

As known, there is a tradeoff between stabilization time and overshoot in PI controller response such that the proportional parameters ($K_{P\omega}$ and K_{Pv}) affect the overshoot, and the integral parameter ($K_{I\omega}$ and K_{Iv}) affect the stabilization time [102]. Hence, predefined ranges for the controller parameters are required to ensure that the response of the system will not violate the prescribed operation limits for the MG frequency and voltage. The limits for the controllers' parameters have been determined by trial and error during the simulation and observing the optimal parameter values that do not adversely jeopardize the response of the system.

4.2.2 The Proposed Control Methodology

The proposed hybrid optimization approach is based on the DEO and ANN techniques. The DEO is a powerful stochastic optimization technique that is distinguished by its simplicity and robustness. Besides, it can solve complex nonlinear problems and converge fast to the optimal solution. The DEO is a population-based optimization algorithm which operates through similar computational steps as employed by a standard evolutionary algorithm. The EA uses iterative progress, such as growth or development in a population that is selected in a guided random search using parallel processing to achieve the desired objective. Contrasting other EA methods, the DEO is very immune against falling into local optimums and has less setting parameters [103].

The setting parameters of the DEO technique are presented in Table 4.3. The optimal generation number and population size are determined by experience and by trial and error during the simulation. Figure 4.6 and Figure 4.7 show the convergence of the two objective functions (4.5) and (4.6) over 100 generations for different levels of disturbances from 1 p.u to 4 p.u. It can be observed from the two figures that the selected setting parameters for the DEO algorithm ensure that the optimal solution is reached for both objective functions.

Table 4.3. The DEO algorithm parameters.

Parameter description	Value
Generation number	100
Population size	50
Mutation factor	0.5
Crossover factor	0.7

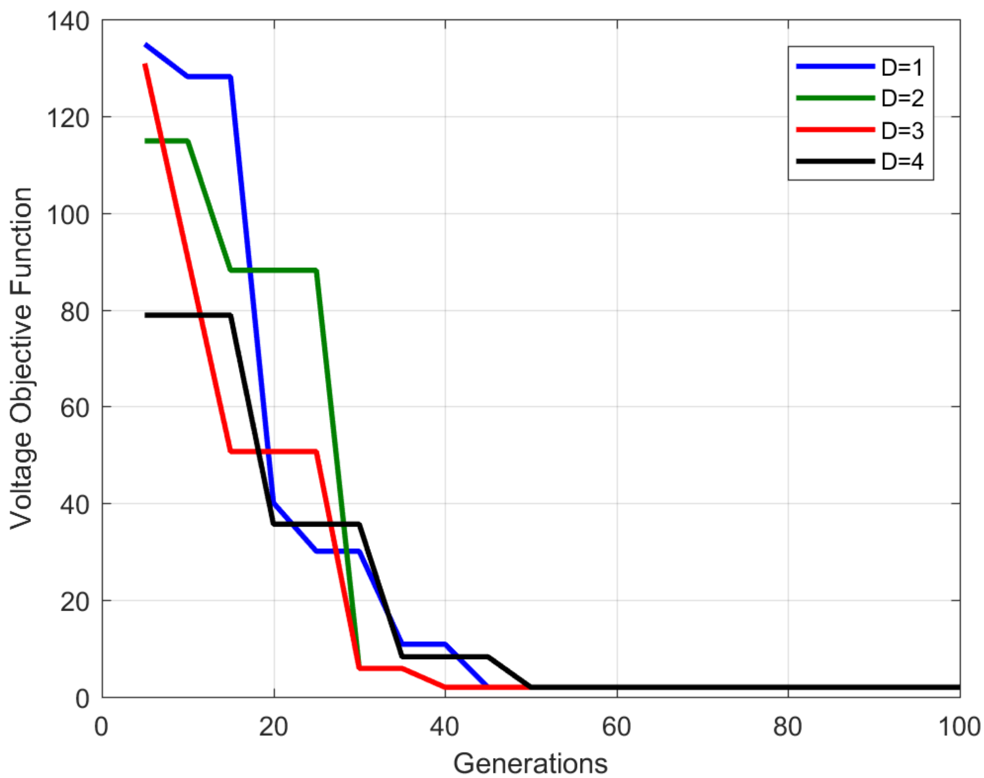

Figure 4.6. The convergence of voltage objective function to the optimal solution.

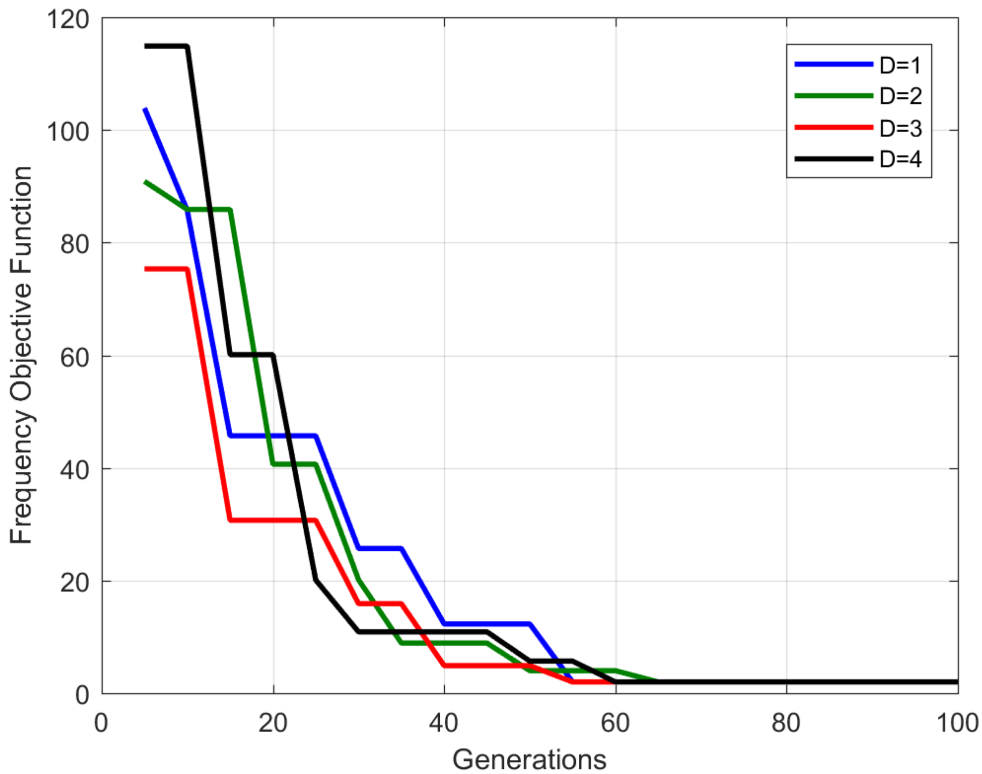

Figure 4.7. The convergence of frequency objective function to the optimal solution.

The flow chart in Figure 4.8 describes in detail the DEO technique. After Appling a disturbance, the DEO algorithm starts first with an initial population of 50 solutions (i.e., controllers' parameters) that have been randomly initialized. Then, the objective functions are calculated as per the expressions (4.5) and (4.6) for all the randomly initialized controllers' parameters. The best parameters that give the minimum voltage ISE and frequency ISE values are searched and saved. Each population undergoes a mutation and crossover process in order to get new generations, and the best solutions are searched again and saved. In doing so, the algorithm checks the stopping criteria, which is reaching up to 100 generations that is the maximum generation number in this optimization technique. Finally, when the stopping criteria is reached, the algorithm stops and gives the optimal parameters for the two decoupled PI controllers.

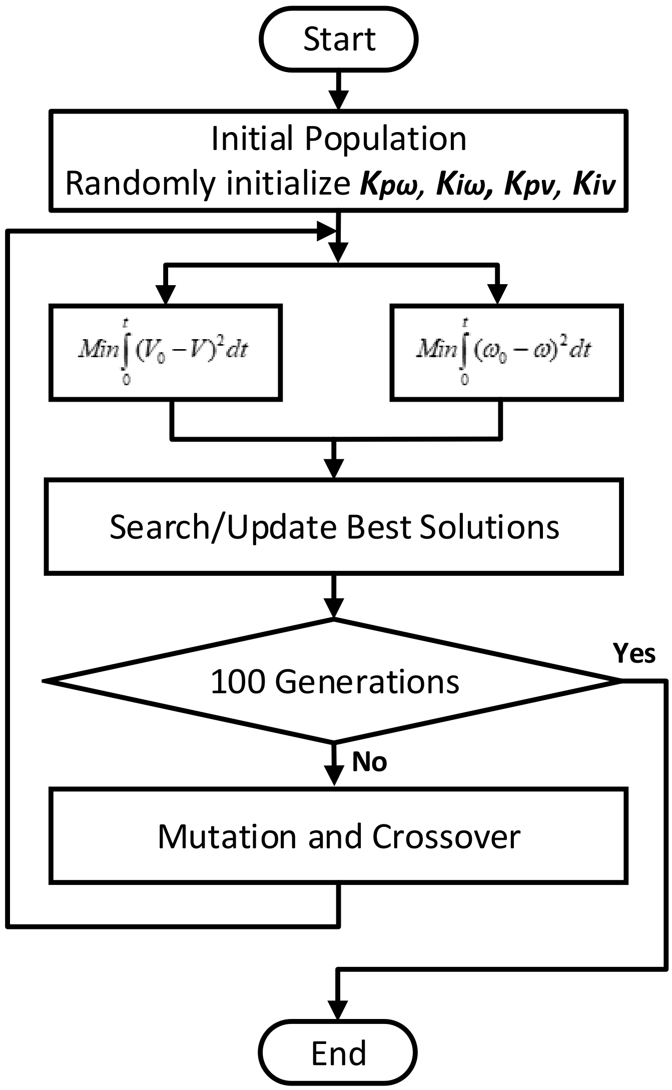

Figure 4.8. The DEO algorithm.

The proposed hybrid DEO and ANN approach is described in **Algorithm 1**. The algorithm starts with applying a disturbance level ranging from 0.1 p.u to 4 p.u. in steps of 0.013 p.u to the MG system. In this proposal, 300 levels of disturbances have been applied. These disturbances simulate sudden changes in the input mechanical torque of the SG. After that, the algorithm runs the DEO to find optimum parameters of the two decoupled BESS-based PI controllers for each disturbance level, as described in Figure 4.8. Then, the obtained optimal parameters, as well as the disturbances, are used to develop and train the ANN, as shown in Figure 4.9. The input to the ANN is the disturbance levels, and the output of the ANN is the optimal controllers' parameters. The developed network consists of one input layer, one hidden layer with 300 neurons, and one output layer with four neurons. This kind of ANNs called a multi-layer feed-forward neural network (MLFFNN), which is the most popular structure of ANNs. Moreover, the constructive technique is used to construct the hidden layer neurons of the developed ANN. The activation functions for the hidden neurons and the output neurons were the commonly used functions, i.e., the tangent sigmoid and the linear function, respectively. The backpropagation training function "trainlm" in the ANN toolbox in MATLAB has been implemented to train the ANN for each operating condition. This training function compares the obtained controller outputs with the targeted outputs. Then, the error signal is propagated back to adjust the ANN weighting matrices and biases, according to Levenberg-Marquardt (LM) optimization [104]. The training process continues until getting the optimal ANN that can identify the optimal controllers' parameters for any disturbance level within the training range.

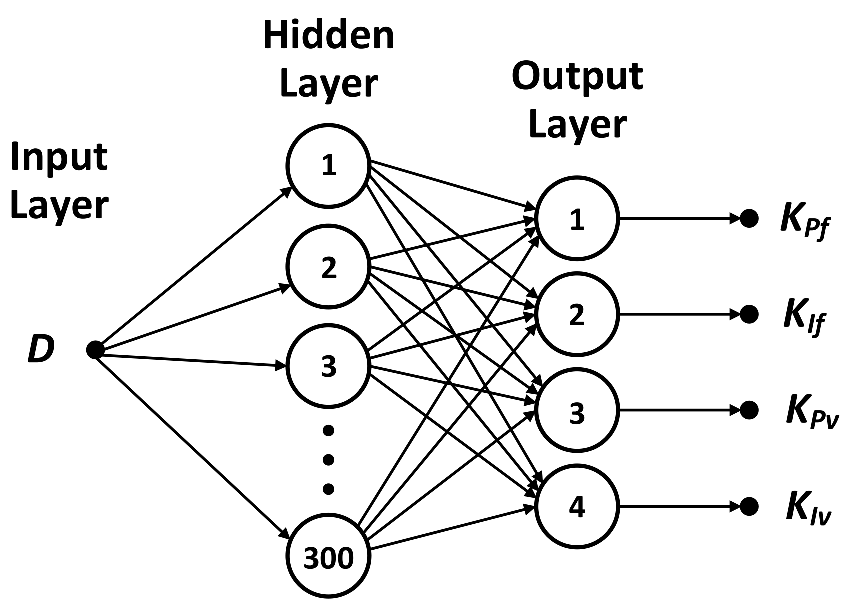

Figure 4.9. The developed ANN.

Algorithm 1. The proposed hybrid DEO and ANN technique

Start

Applying a disturbance level (D)

$D = 0.1$

While $i \leq 300$ do

- **Saving the disturbance level**

$D \rightarrow Input\_Vector$

- **Running the DEO algorithm as per Figure 4.8**

Initialization of $K_{P\varpi}, K_{Pv}, K_{I\varpi}, K_{Iv}$

Calculation of objective functions (4.5) and (4.6)

Mutation and crossover

Getting the optimal $K_{P\varpi}, K_{Pv}, K_{I\varpi}, K_{Iv}$

- **Saving the optimal controllers' parameters**

$K_{P\varpi}, K_{Pv}, K_{I\varpi}, K_{Iv} \rightarrow Output\_Vectors$

$D = D + 0.013$

End while

- **Developing the ANN as per Figure 4.9**

Training the ANN with:

$Input\_Vector$ & $Output\_Vectors$

Generating the training performance curves

Saving the trained ANN.

- **Testing the hybrid DEO and ANN technique**

Applying a new level of Disturbance

Plot MG voltage and frequency response curves

End

Figure 4.10 and Figure 4.11 show the training data fit and performance curves of the developed artificial neural network, respectively. The training data (in black circles) shown in Figure 4.10 are perfectly fit in the regression line (in blue) with correlation factor R=1. Additionally, it can be observed from Figure 4.11 that the best training performance found to be at Epoch number **5** with MSE converges to zero, which indicates that the developed ANN is well trained.

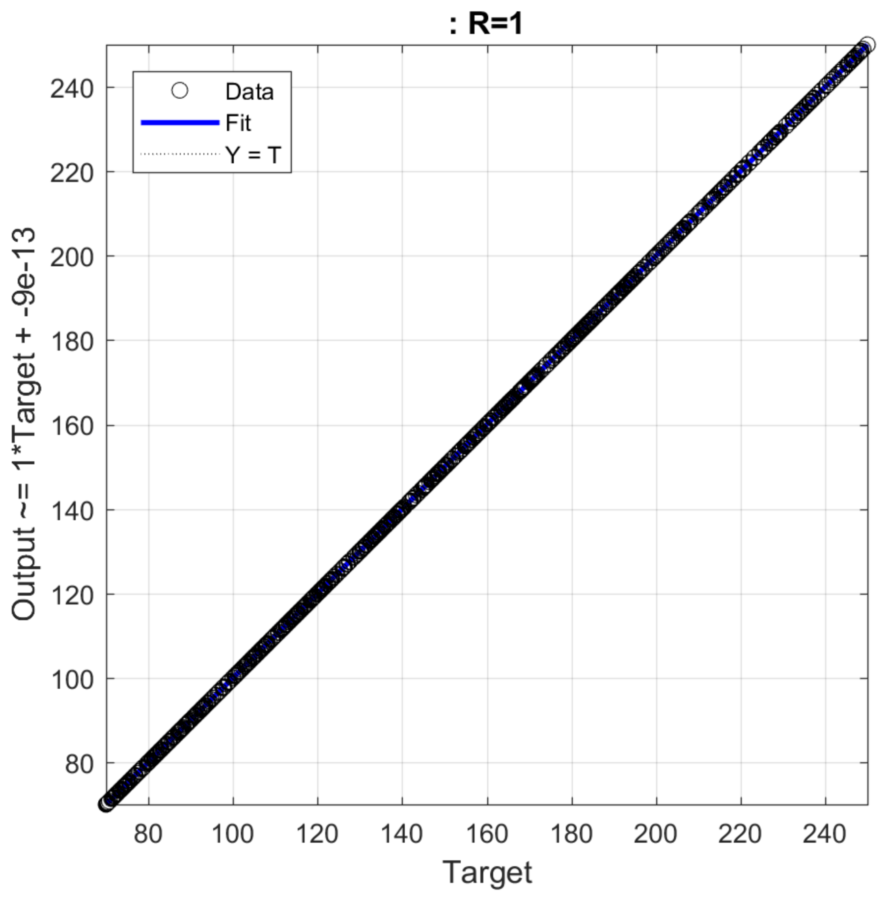

Figure 4.10. The ANN training data fit.

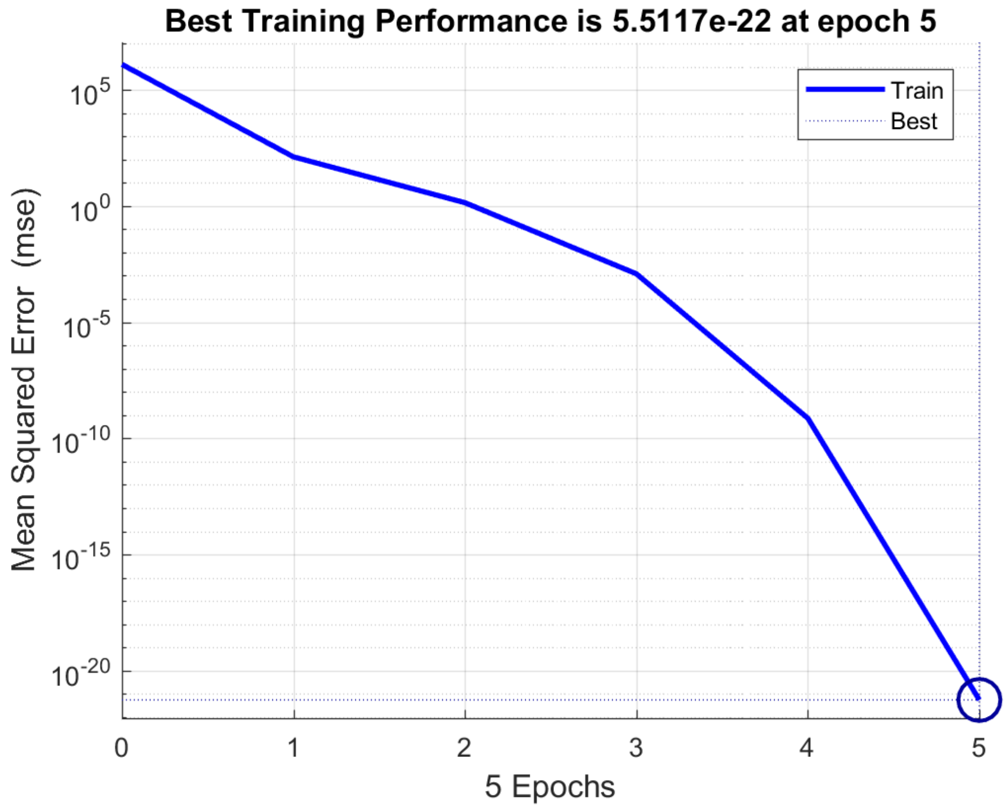

Figure 4.11. The ANN training performance curve.

CHAPTER 5

RESULTS AND DISCUSSIONS

This chapter discusses in detail the simulation results for the two proposed intelligent control approaches. The first section presents the single BESS-based controller performance results for low level disturbances. Whereas, the second section discusses the performance results of the double BESS-based control approach.

5.1 Single BESS-Based Controller

After training of the ANN, a random disturbance between [0.2~0.8 p.u] has been generated (0.3135 p.u) in order to verify the performance of the trained ANN. The input disturbance entered into the ANN, and then the output controller parameters are obtained, as shown in Table 5.1 without violating the specified controller parameters' constraints.

Table 5.1. PI controller parameters.

Controller parameter	Value
Kp	128.22
Ki	161.78

The dynamic responses of the system with and without the action of the controller along with the comprehensive comparison for the proposed DEO-ANN controller and the well-known benchmark classical PID controller are shown in the following Figures. In fact, the PID controller is widely used as a benchmark controller, and many papers in the literature compare the performance of their proposed controllers with the performance of the PID controller [31-35]. The PID block in MATLAB SIMULINK has been utilized, which has the control formula in (5.1). The PID controller parameters have been tuned using the well-known Ziegler-Nichols (ZN) method [102].

$$PID\_Control\_Signal = K_P \times e(t) + K_i \times \int_0^t e(t)dt + K_D \times \frac{d}{dt}e(t) \qquad (5.1)$$

Figure 5.1 and Figure 5.2 demonstrate the performance comparison of the proposed DEO-ANN controller using the obtained controller parameters from the developed ANN. It can be observed that the proposed controller performs better than the benchmark model in terms of stabilization time to restore the MG system frequency and voltage to the normal operating condition within a period of 1.5 seconds.

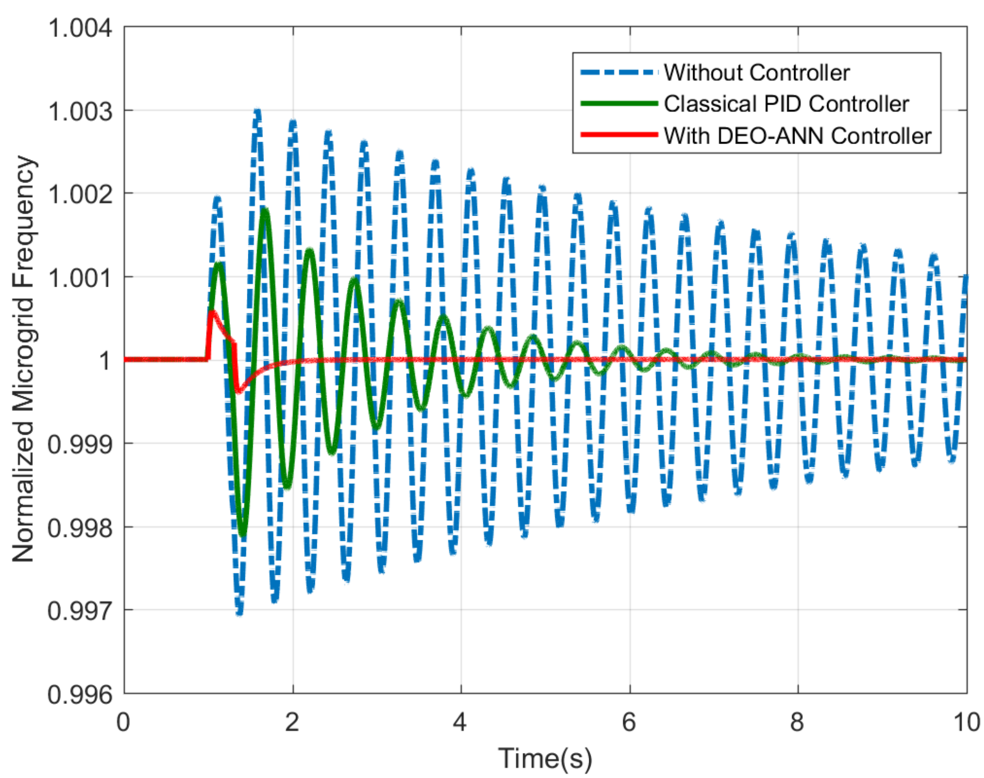

Figure 5.1. MG system frequency (in p.u.).

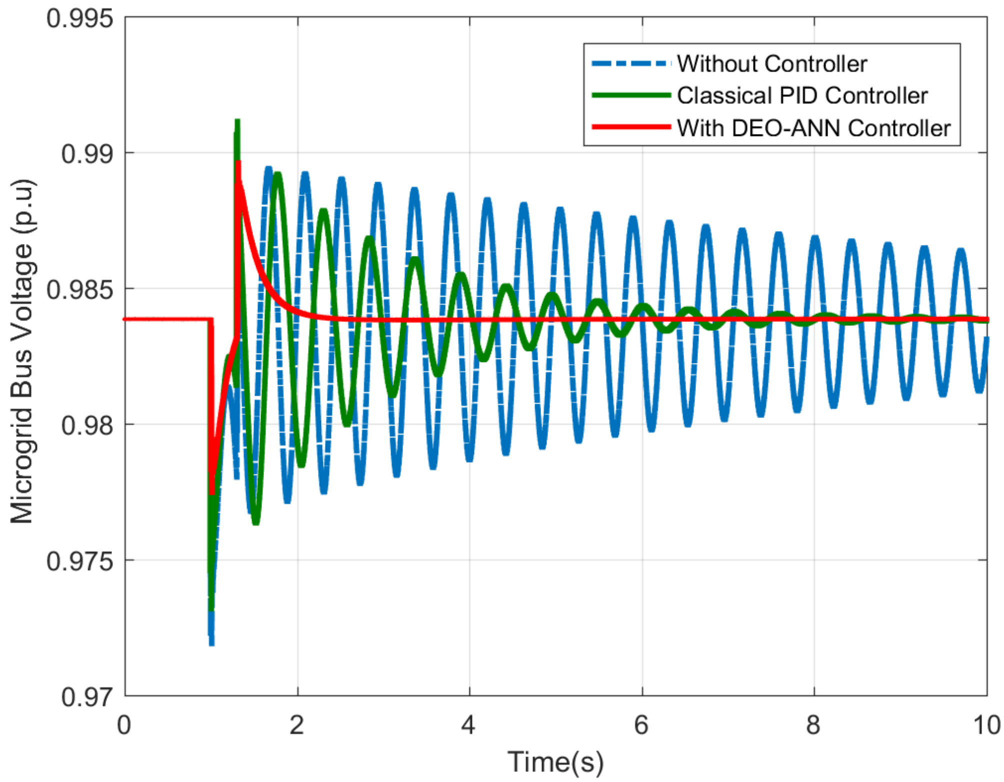

Figure 5.2. MG system voltage (in p.u.).

The variations in the DSG internal voltage and the DSG field voltage are shown in Figure 5.3 and Figure 5.4, respectively. It can be observed that in the absence of the control action, the oscillations in the DSG internal voltage and field voltage continue for a longer period of time. However, with the action of the intelligent BESS controller, the oscillations are damped quickly and returned to the steady-state condition in 3 seconds for the DSG internal voltage and less than 1.5 seconds for the DSG field voltage.

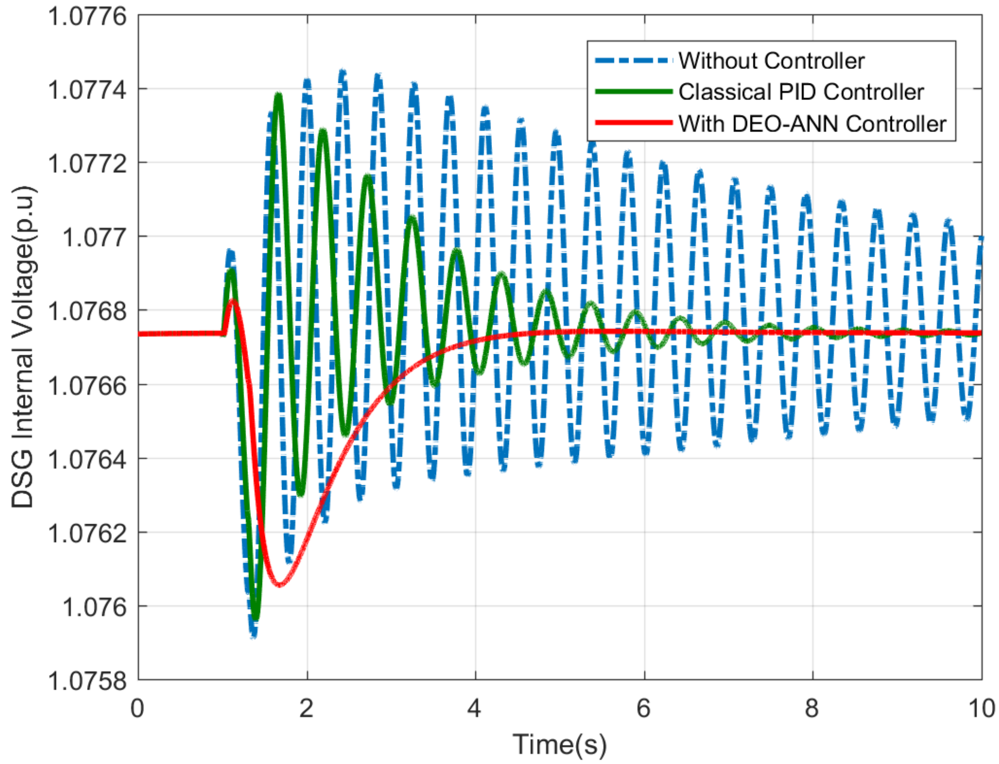

Figure 5.3. DSG internal voltage.

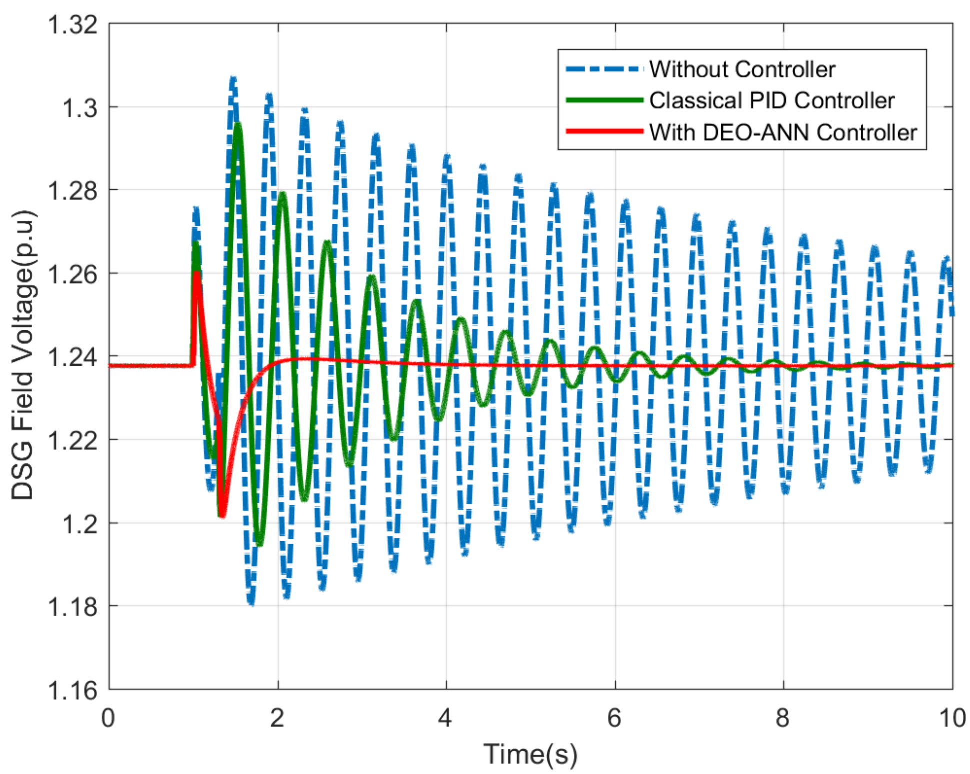

Figure 5.4. DSG Field Voltage.

The transient responses of the PV output current and the DC link output voltage are recorded in Figure 5.5 and Figure 5.6. Without the proposed controller, the PV output current and the DC link output voltage fluctuate for more than 10 seconds. However, with the action of the intelligent BESS controller, the fluctuations are damped quickly, restoring the PV output current and the DC link output voltage to the steady-state condition in less than 2 seconds.

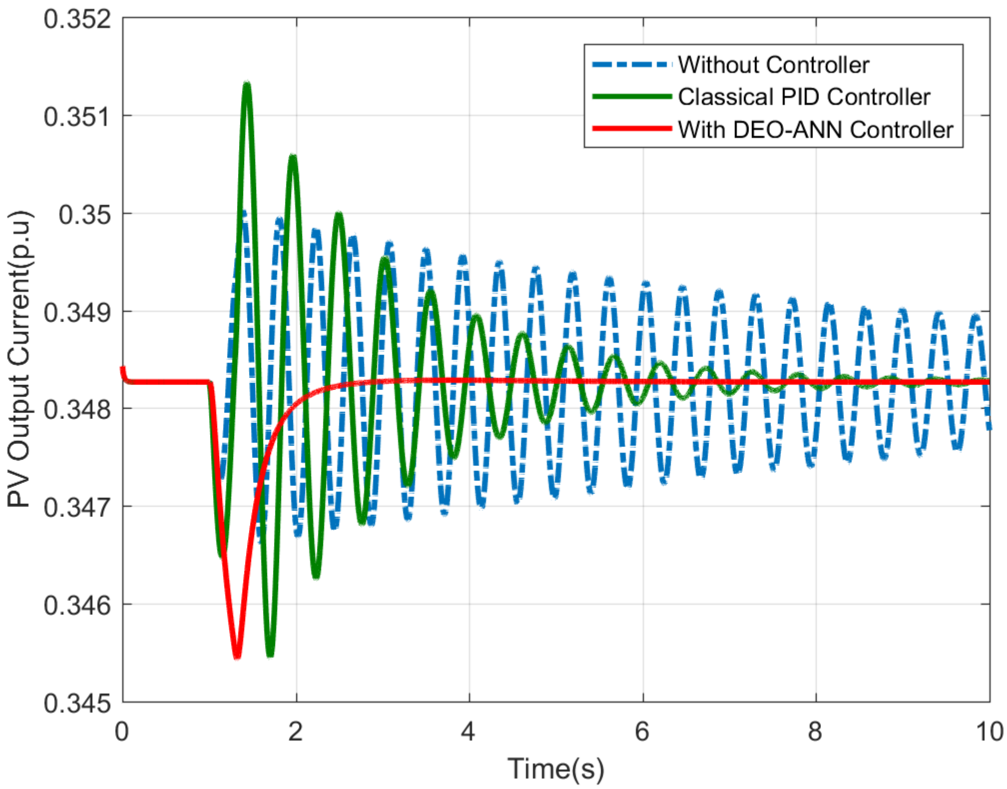

Figure 5.5. PV output current.

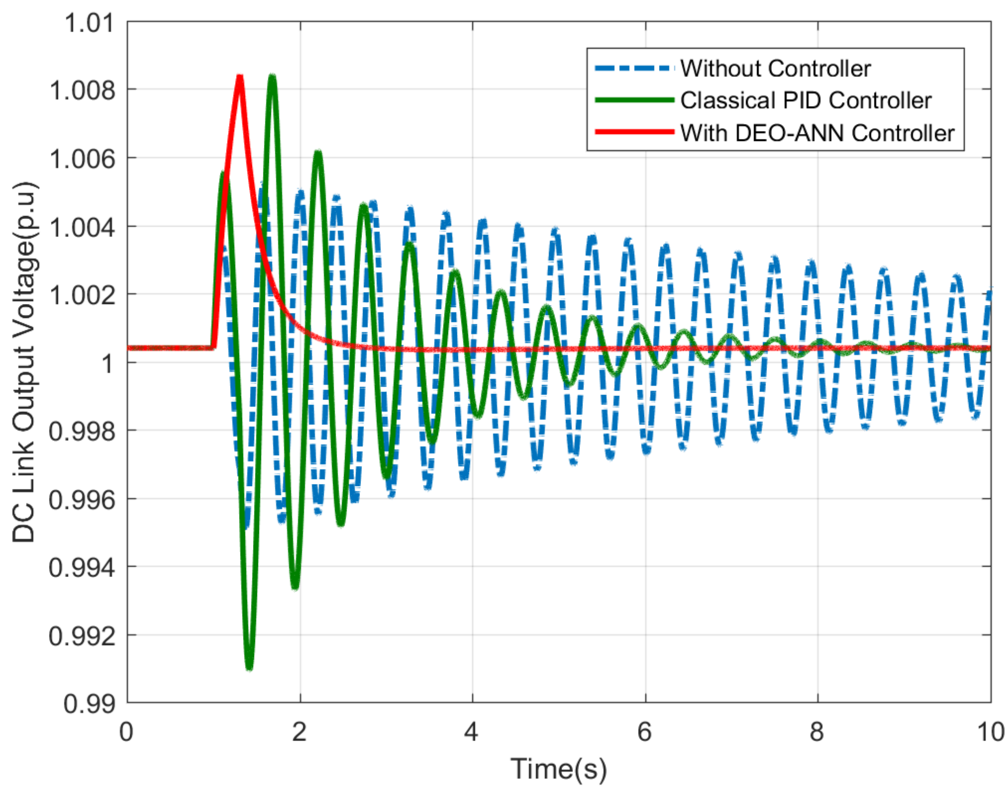

Figure 5.6. DC link output voltage.

Figure 5.7 and Figure 5.8 show the responses of the inverter output current along d-axis and the inverter output current along q-axis, respectively. It can be noticed from these figures that the uncontrolled case leads to continuous oscillations. However, the transient responses with the proposed controller are improved, and the inverter output current along d-axis and q-axis restored to the steady-state condition in less than 1.5 seconds.

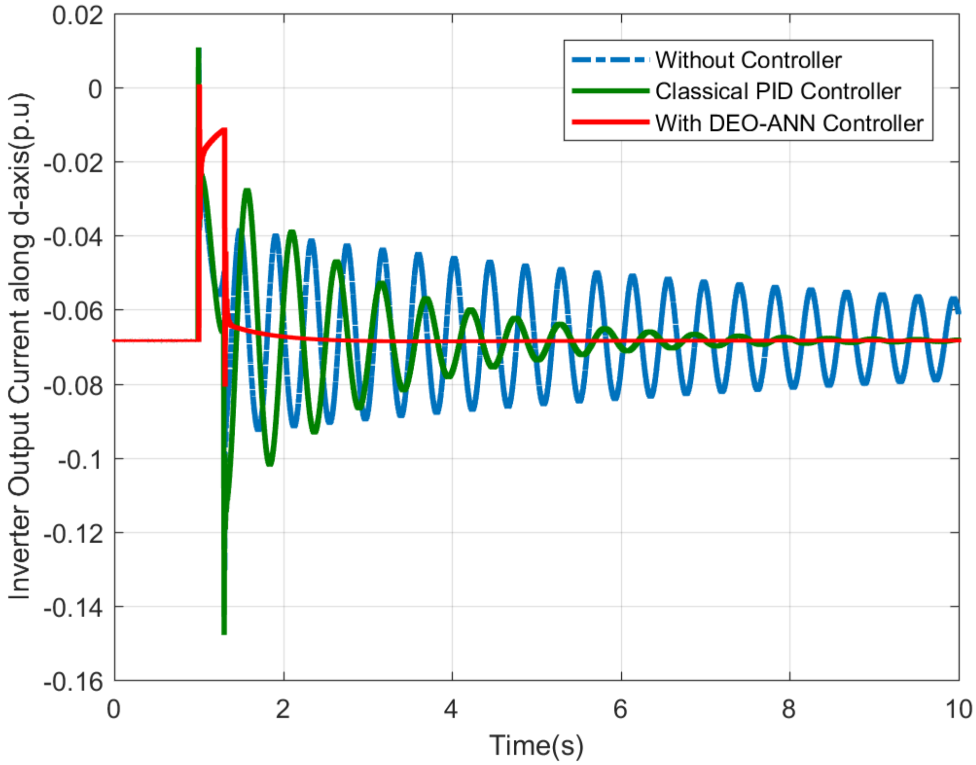

Figure 5.7. Inverter output current along d-axis.

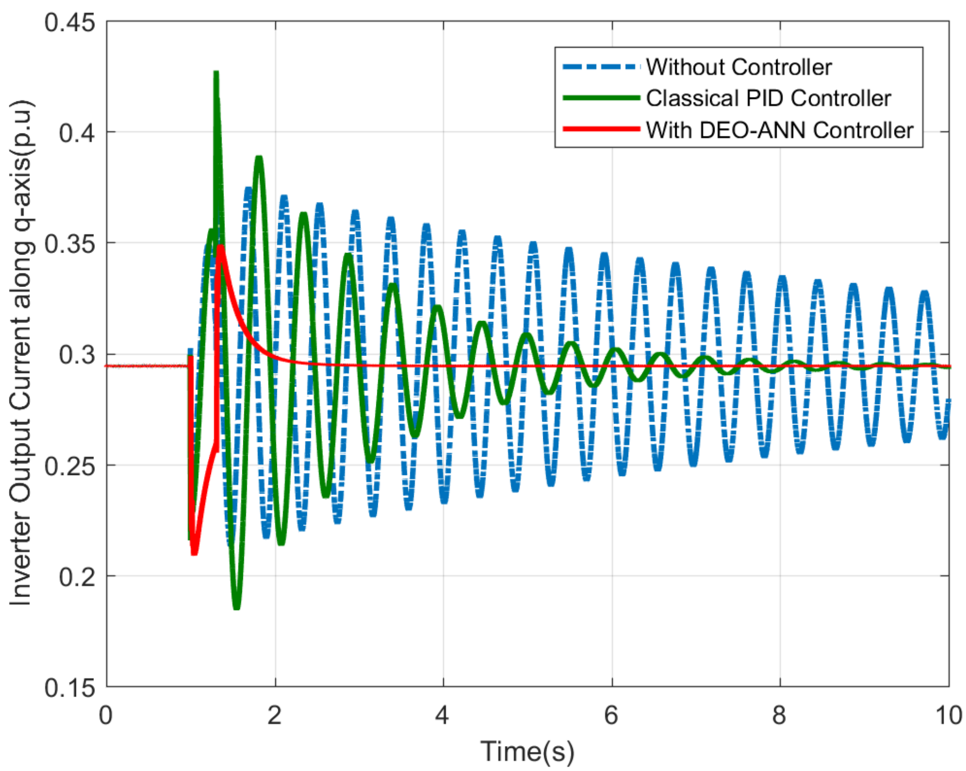

Figure 5.8. Inverter output current along q-axis.

Figure 5.9, Figure 5.10, Figure 5.11, and Figure 5.12 show the transient responses of the LP filer output current along d-axis, the LP filer output current along q-axis, the LP filter capacitor voltage along d-axis, and the LP filter capacitor voltage along q-axis respectively. It can be observed from these four figures that in the absence of the controller action, the oscillations in the LP filter output current along d-axis, the LP filter output current along q-axis, the LP filter capacitor voltage along d-axis, and the LP filter capacitor voltage along q-axis continue for a longer period of time. However, the responses in the presence of controller action are enhanced, and the system returned to the steady-state conditions in less than 1.5 seconds. Moreover, the performance of the proposed DEO-ANN controller surpassed the performance of the classical PID controller in all of the four figures.

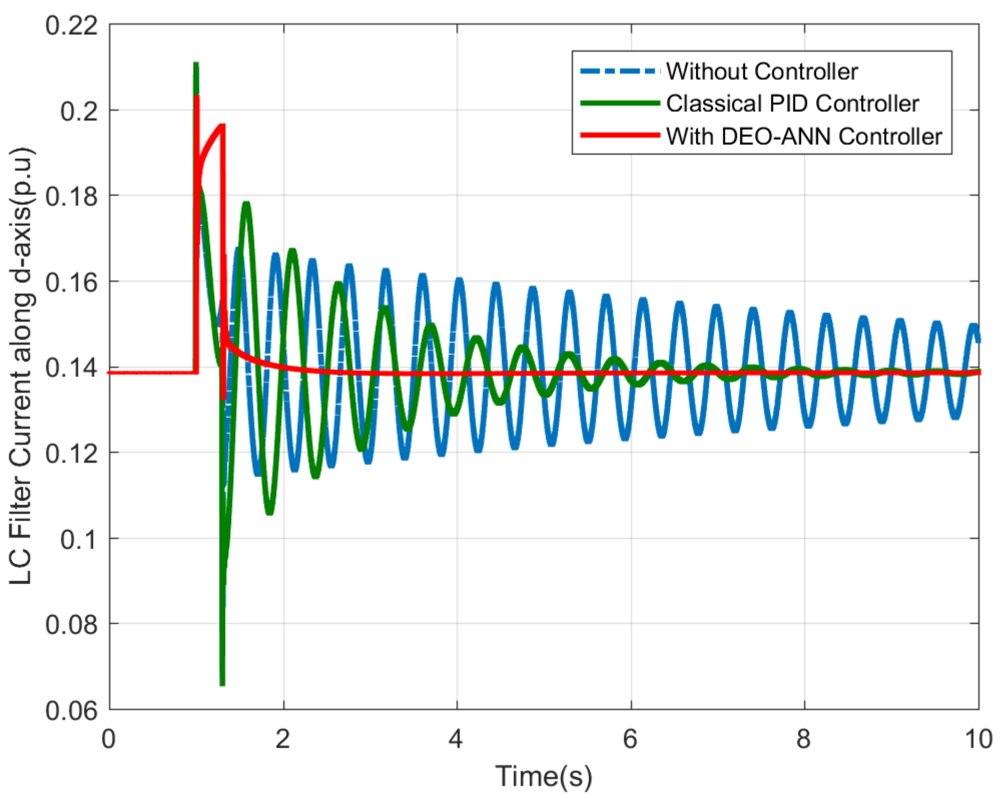

Figure 5.9. LP filter output current along d-axis.

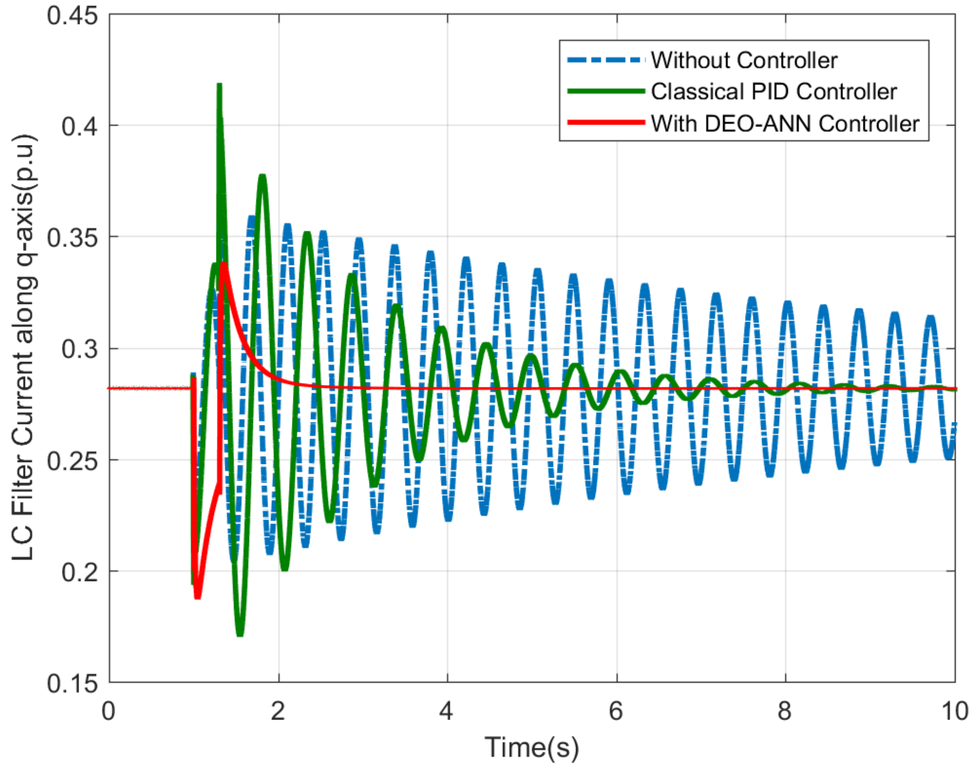

Figure 5.10. LP filter output current along q-axis.

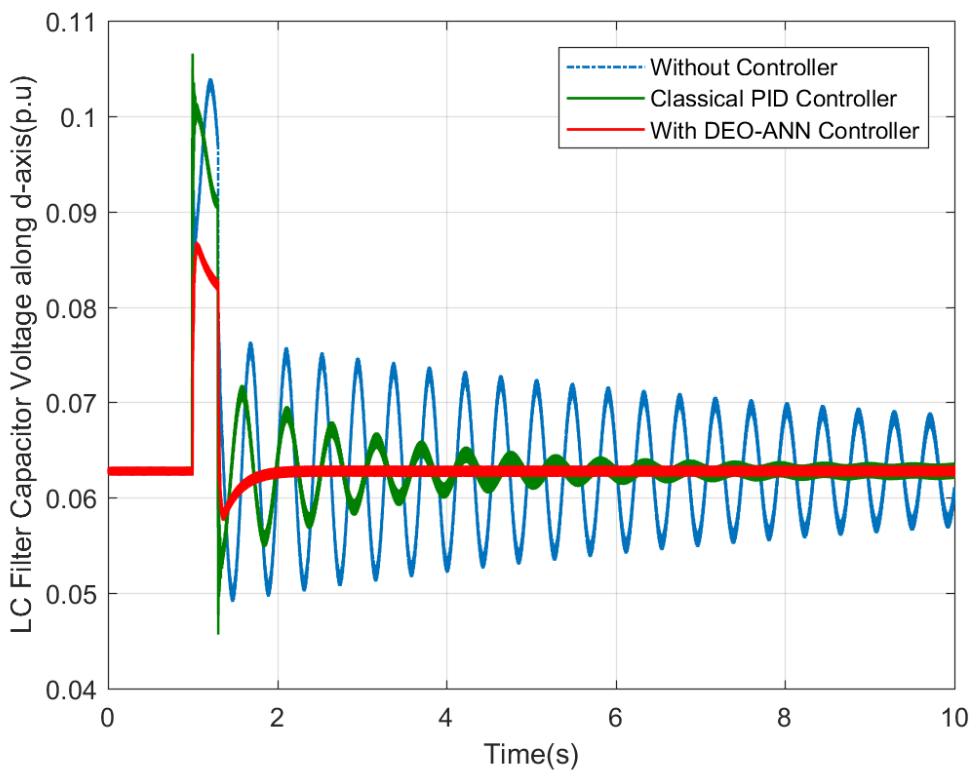

Figure 5.11. LP filter capacitor voltage along d-axis.

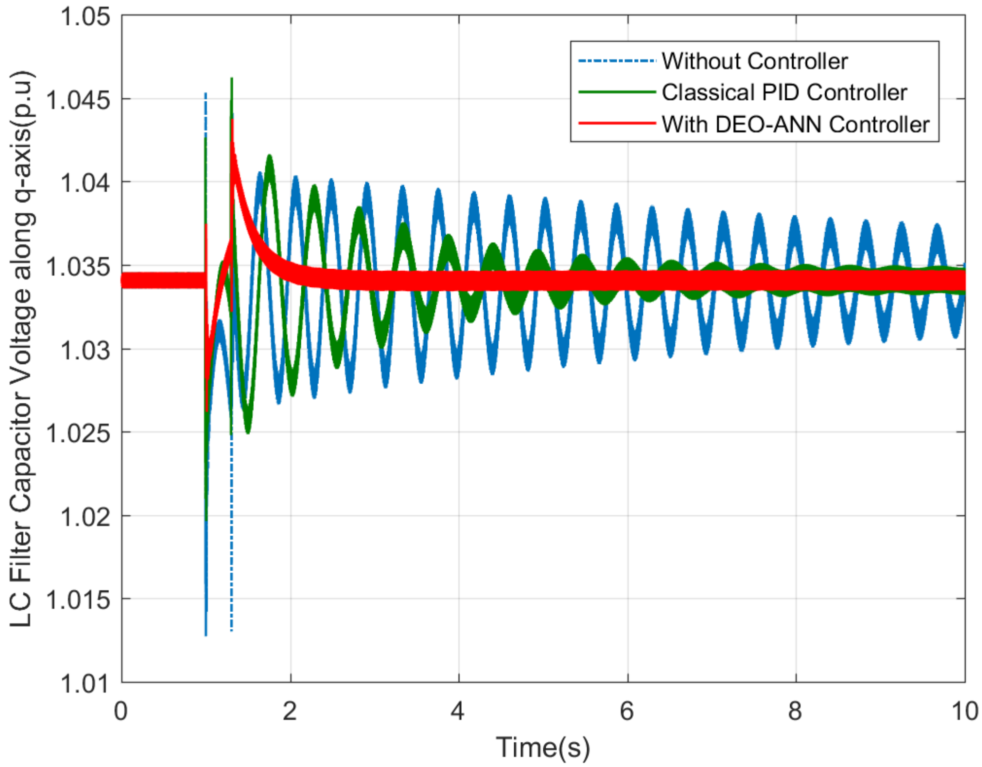

Figure 5.12. LP filter capacitor voltage along q-axis.

Figure 5.13 and Figure 5.14 show the BESS performance during transients with and without the action of the proposed PI controller. The BESS behaves randomly without a proper controller and fluctuates for a long period of time. On the other hand, with the use of the intelligent PI controller, the BESS restored the system to steady-state conditions within 1 second. The sudden changes in the input mechanical torque of the DSG are mitigated by the BESS injection or absorption of real power, as shown in Figure 5.13. This will reduce the amplitude of the oscillations in various MG system quantities, practically the system frequency. Similarly, the variations of the PCC MG voltage during contingencies are reduced by the VSC-interfaced BESS injection or absorption of reactive power, as shown in Figure 5.14. The proposed PI controller has successfully managed the active and reactive power flow from and to the BESS in order to maintain the system frequency and voltage within the prescribed operating limits.

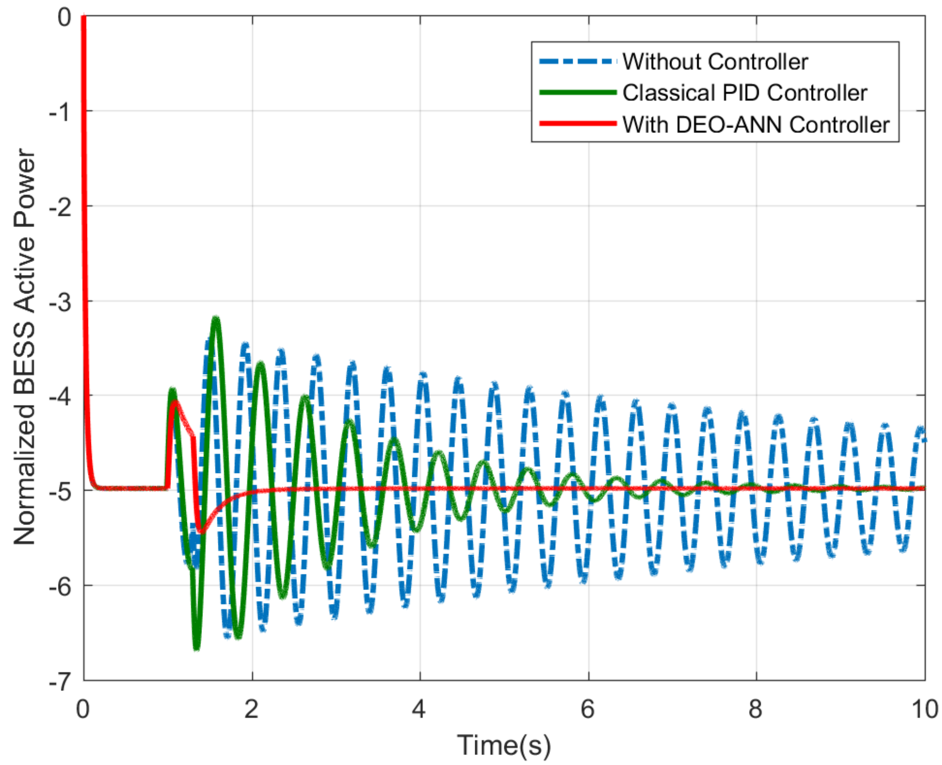

Figure 5.13. Injected real power by the BESS.

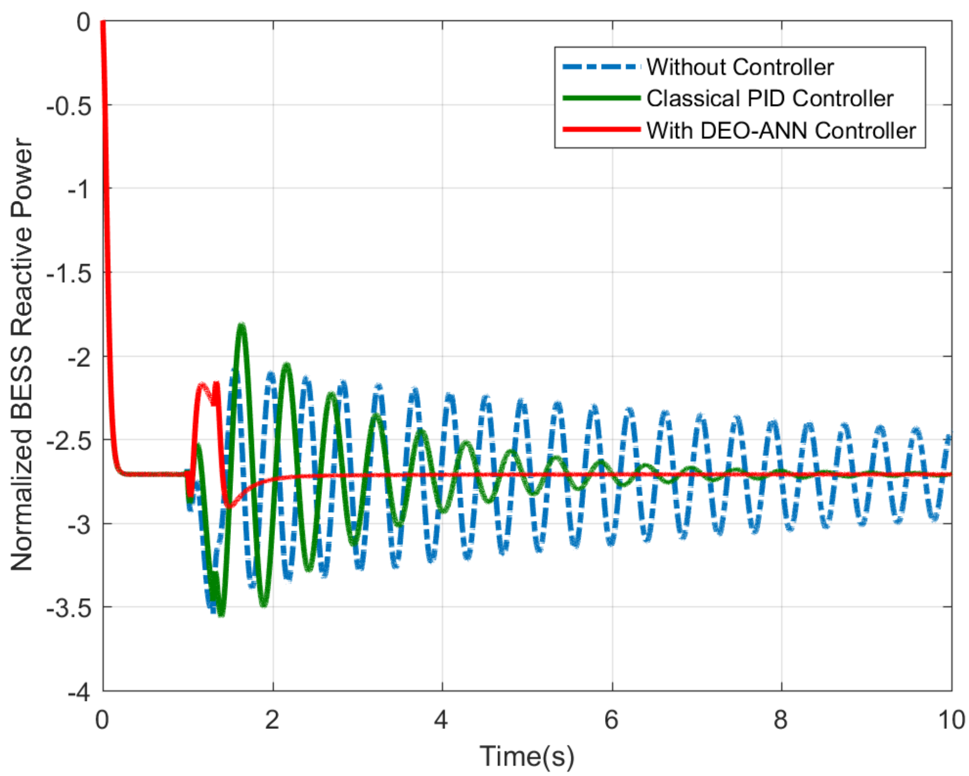

Figure 5.14. Injected reactive power by the BESS.

It can be observed from the simulation results that the proposed DEO-ANN controller performs better in terms of stabilization time and overshoot when compared with the benchmark PID controller in all given scenarios. Although there is a tradeoff between the stabilization time and overshoot, the proposed controller was capable of keeping both the percentage of overshoot along with stabilization time to a minimum level.

5.2 Double BESS-Based Controllers

In order to verify the effectiveness and robustness of the proposed control approach, two randomly generated low-level and high-level disturbances between (0.1 p.u) and (4 p.u) have been applied to the MG system. The dynamic responses of the system with and without the action of proposed controllers along with a performance comparison with the well-known benchmark PID controller are provided in the following subsections.

5.2.1 At Low-Level Disturbances

A random low magnitude disturbance has been generated (0.512 p.u) and applied to the MG system. The proposed two decoupled controllers have generated the optimal controllers' parameters, as shown in Table 5.2.

Table 5.2. Optimal parameters at low-level disturbances.

Controller parameter	Value
$K_{P\omega}$	73.28
$K_{I\omega}$	146.39
K_{Pv}	61.74
K_{Iv}	121.58

Figure 5.15 and Figure 5.16 show the dynamic responses of the MG system frequency and voltage with the action of the proposed DEO-ANN decoupled controllers (in red), the PID controller (in blue), and without controller actions (in dotted green). It can be observed that in the absence of the control action, the oscillations in the MG system frequency and voltage continue for a more extended period of time. However, with the action of the proposed DEO-ANN controllers, the oscillations are damped quickly and returned to the steady-state condition in less than 2 seconds. Furthermore, the proposed DEO-ANN controllers performed better than the PID controller in terms of stabilization time and overshoot.

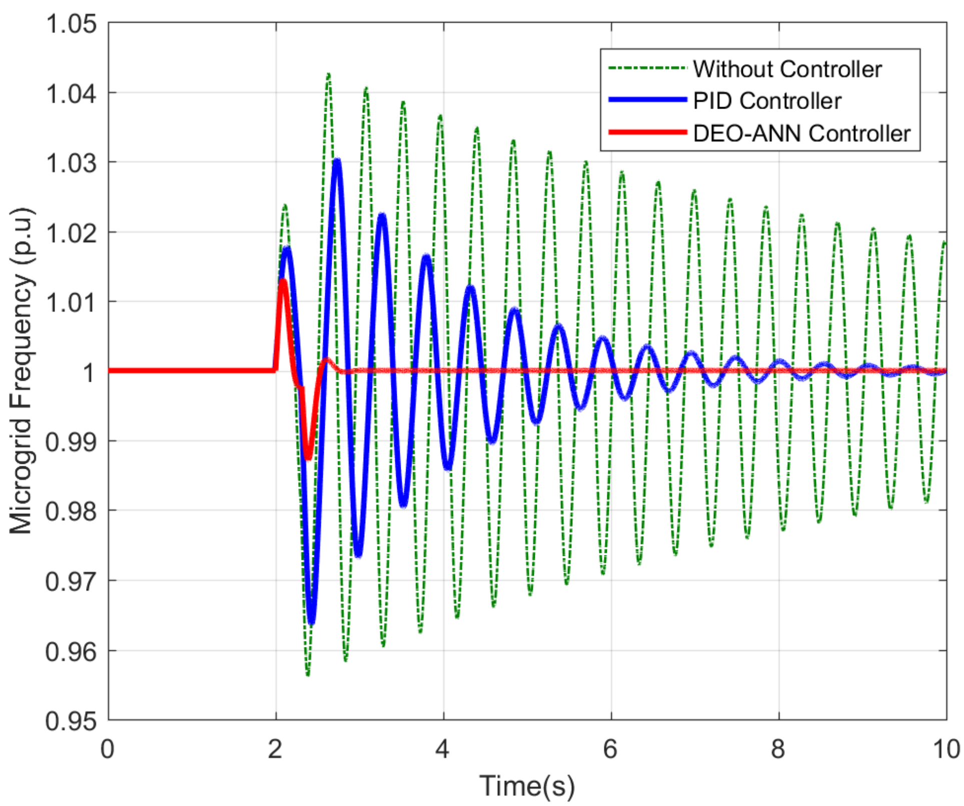

Figure 5.15. The MG frequency.

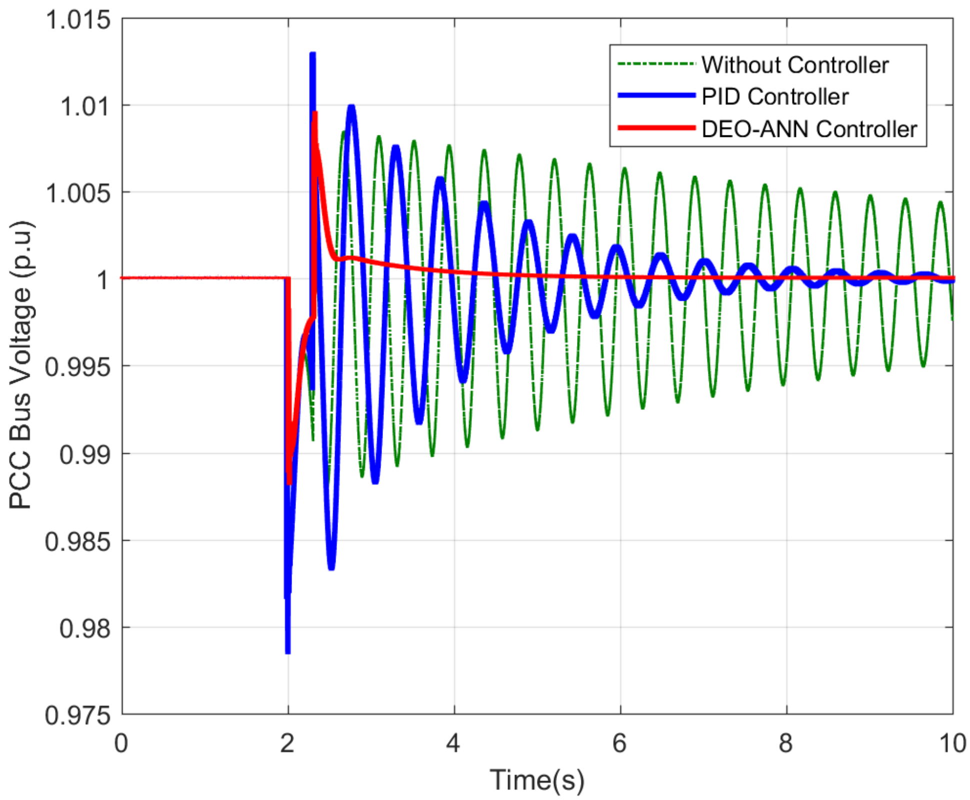

Figure 5.16. The MG PCC bus voltage.

The BESS mitigates the oscillations of the MG system quantities by injecting or absorbing the required amount of active and reactive power properly. The active power contributes to frequency stability, and the reactive power recovers the MG voltage to normal conditions. Thus, the MG system's overall power quality is improved. Figure 5.17 and Figure 5.18 show the BESS dynamic performance subjected to the applied disturbance level with and without the action of the proposed DEO-ANN controllers as compared with the PID controller response. As can be observed, without appropriate control, the BESS active and reactive power fluctuate for an extended period of time. Whereas, with the presence of the proposed DEO-ANN controllers, the BESS restored the system to normal operating conditions also in about 1.5 seconds.

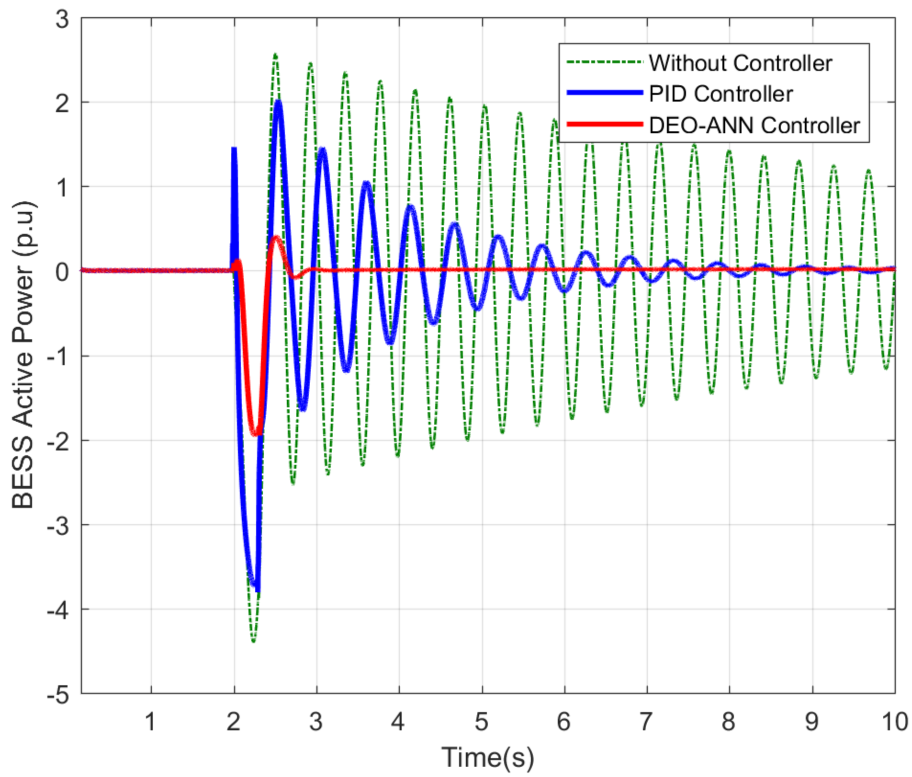

Figure 5.17. The BESS injected active power.

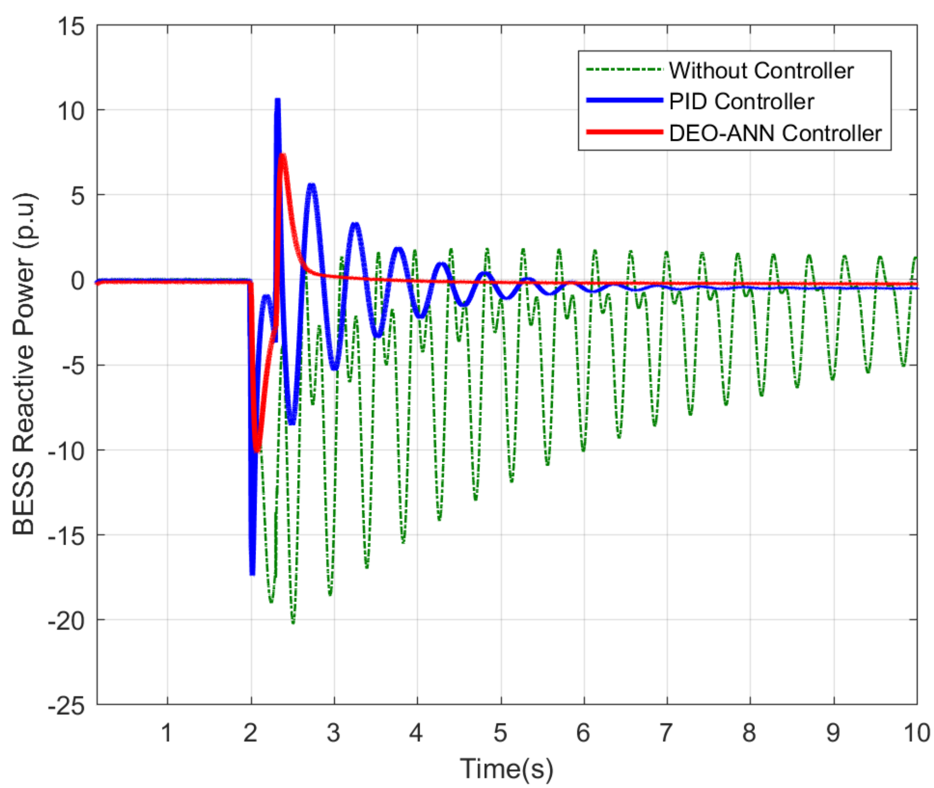

Figure 5.18. The BESS injected reactive power.

Moreover, the proposed DEO-ANN controllers achieved superior performance over the PID controller in both stabilization time and overshoot. Therefore, the effectiveness of the proposed control approach has been verified under low-level disturbances.

5.2.2 At High-Level Disturbances

In order to verify the robustness of the proposed two decoupled controllers, a random high magnitude disturbance has been generated (3.287 p.u) and applied to the MG system. The optimal parameters generated by the two proposed controllers are shown in Table 5.3.

Table 5.3. Optimal parameters at high-level disturbances.

Controller parameter	Value
$K_{P\omega}$	91.13
$K_{I\omega}$	173.22
K_{Pv}	78.06
K_{Iv}	156.41

Figure 5.19 and Figure 5.20 show the variations in the MG system frequency and voltage, respectively. It can be observed from these two figures that without a control action, the MG system frequency and voltage oscillate for more than 10 seconds. However, the proposed DEO-ANN controllers restored the system to the steady-state condition in less than 2 seconds. Additionally, the proposed DEO-ANN controllers achieved less stabilization time and response overshoot as compared with the PID controller.

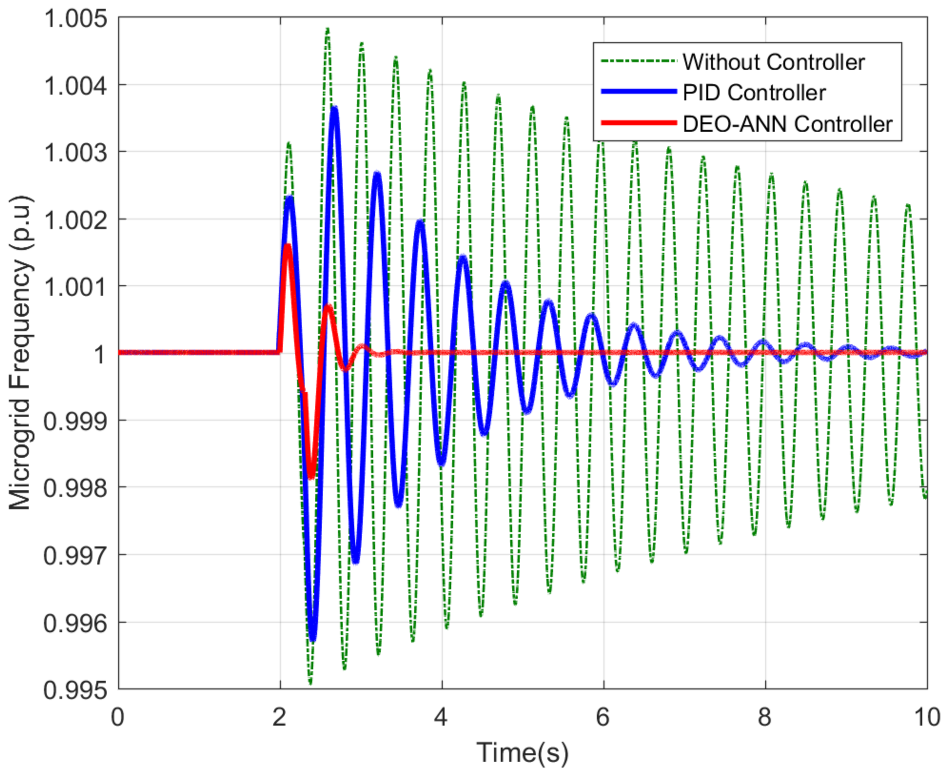

Figure 5.19. The MG frequency (in p.u.).

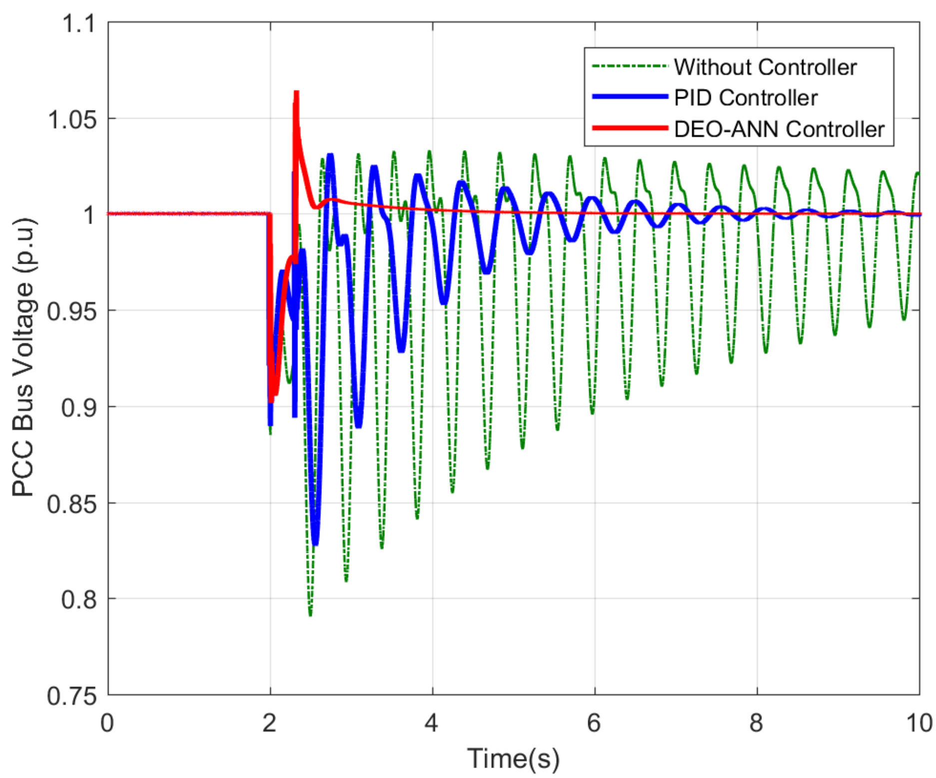

Figure 5.20. The MG PCC bus voltage (in p.u).

In order to show the superiority of the proposed control approach at critical disturbances, the proposed controller has been compared with the PID controller in terms of the following performance indices; Integral of Absolute Error (IAE), ISE, Integral of Time multiplied Squared Error (ITSE), Integral of Time multiplied Absolute Error (ITAE), overshoot (OV), and settling time (ST). These indices are the most performance measures that are considered in control design [105].

Table 5.4 and Table 5.5 show a quantitative comparison between the performance of the proposed DEO-ANN controller and the PID controller for the MG frequency and voltage response. It can be observed that at critical disturbances, the proposed controllers surpassed the PID controller in all the performance measures.

Table 5.4. Performance indices of MG frequency response.

Performance Index	**The DEO-ANN Controller**	**The PID Controller**
IAS	6.76×10^{-4}	1.90×10^{-2}
ISE	9.66×10^{-4}	0.0242
ITSE	2.16×10^{-7}	5.31×10^{-4}
ITAE	1.55×10^{-6}	6.24×10^{-3}
OV (%)	1.55	3.5
ST (s)	1.12	5.34

Table 5.5. Performance indices of MG voltage response.

Performance Index	The DEO-ANN Controller	The PID Controller
IAS	1.6×10^{-3}	0.073
ISE	2.13×10^{-4}	6.74×10^{-2}
ITSE	5.55×10^{-6}	2.37×10^{-3}
ITAE	4.87×10^{-6}	7.06×10^{-2}
OV (%)	1.25	2.21
ST (s)	1.96	7.11

Figure 5.21 and Figure 5.22 show the BESS dynamic performance subjected to the applied high magnitude disturbance in the presence and absence of the controllers' actions.

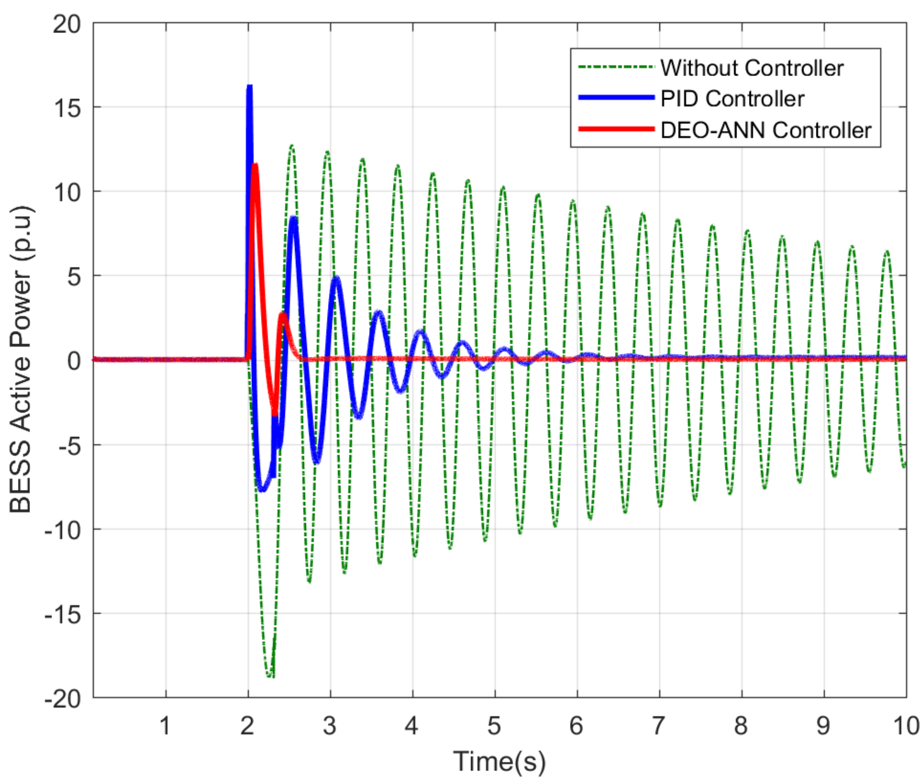

Figure 5.21. The BESS injected active power.

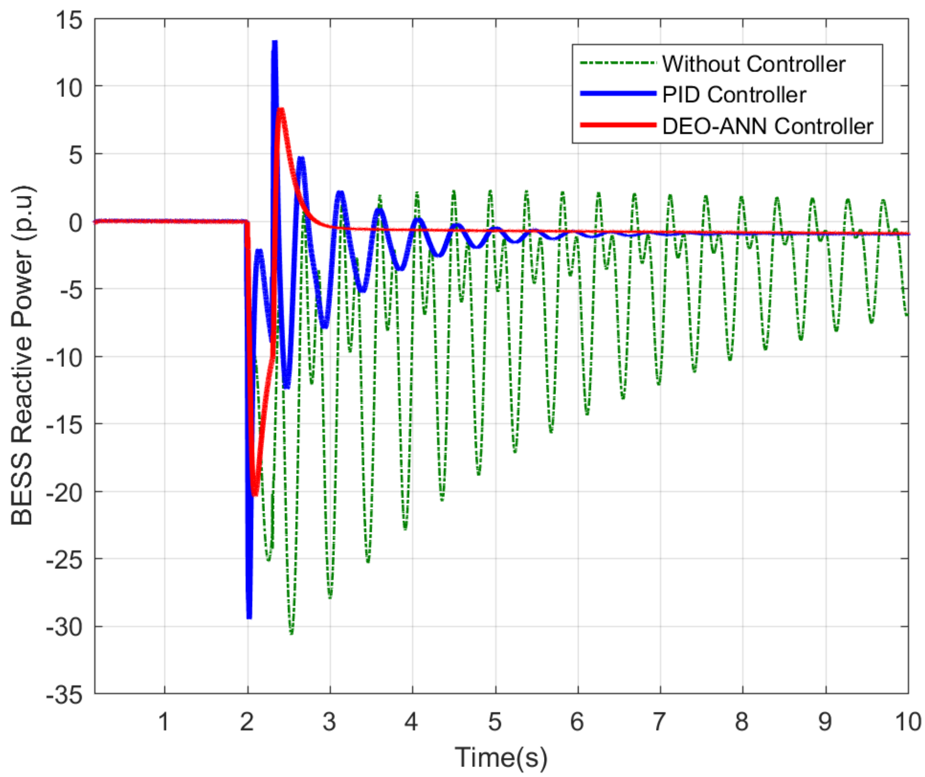

Figure 5.22. The BESS injected reactive power.

It can be noticed that the uncontrolled case leads to continuous oscillations in the BESS active and reactive power. However, the dynamic responses with the proposed DEO-ANN controllers are improved, and the BESS active and reactive power restored to normal operating conditions in less than 2 seconds.

Furthermore, the proposed DEO-ANN controllers have also achieved better performance at higher magnitude disturbances as compared with the PID controller in both stabilization time and overshoot. Hence the robustness of the proposed control approach has been verified under high magnitude disturbances. It can be observed from the simulation results that the proposed DEO-ANN controllers have successfully managed the active and reactive power flow from and to the BESS in order to improve the MG power quality. Furthermore, the proposed DEO-ANN controllers performed better in terms of all the performance indices when compared with the benchmark PID controller. Moreover, the proposed DEO-ANN controllers in all the given disturbance scenarios were capable of keeping both the percentage of overshoot along with stabilization time to the minimum level without violating the prescribed constraints. Hence, the simulation results have proven the effectiveness and robustness of the proposed control approach.

5.3 A Comparative Study Between the Two Proposed Approaches

The following summarized points can be observed from the simulation results of the single BESS-based controller and the double BESS-based controllers presented in last to sections:

- The Double BESS-based controller approach is robust for low and critical unknown random disturbances (between 0 to 4 p.u.) in Microgrids. In contrast, the Single BESS-based controller approach is applicable only for low-level disturbances (less than 1 per unit).
- The maximum generation number of the DEO technique used in the Single controller approach is 50, whereas the DEO generation number in Double controller approach is, which indicates that the DEO in Single controller approach converges faster to the optimal solution as compared with the DEO used in Double controller approach.
- The hidden layer of ANN utilized in the Double controller approach consists of 300 neurons. Whereas, the hidden layer of the ANN used in Single controller approach consists of 200 neurons. That means the training time of the ANN used in Double controller approach is longer than the training time of the ANN used in the Single controller approach.

CHAPTER 6

CONCLUSION AND FUTURE WORK

6.1 Conclusion

Distributed generation systems have attracted a lot of attention with the growth of microgrids and the emerging global trend towards renewable energy resources. However, the intermittent nature of such generations poses challenges, especially for power quality such as frequency and voltage variations at the point of common coupling. Microgrids provide the flexibility to integrate renewables into the power network. Nevertheless, the transience and unpredictability of most renewable energy sources exacerbate the power quality of the grid network. The deployment and optimal utilization of energy storage systems, to act as an energy buffer are hence pertinent.

In this thesis, two intelligent BESS-based control approaches have been proposed to improve the power quality of a MG system; in particular, voltage control and frequency regulation at steady-state conditions are targeted. The proposed control strategies are based on the combination of two key techniques, DEO and ANN, thus making a hybrid control system actually to benefit from complementary benefits of both approaches. To the best of author's knowledge, the proposed approaches in this thesis have not been introduced earlier in the literature. The frequency and voltage at the PCC bus of the MG have been maintained within prescribed operating limits during normal and transients' conditions. The first proposal utilized a single BESS-based controller, whereas, the second proposal utilized two decoupled BESS-based controllers. The MG system considered in this research was consisting of two distributed generators, a diesel synchronous generator, and a photovoltaic power system, integrated with a BESS. The detailed nonlinear equations that represent the dynamic model of the MG system have been provided. The controller parameters have been optimized using the DEO technique under different disturbance levels. Consequently, the optimized controller parameters and the corresponding disturbances are arranged in input and output patterns to train the ANN. Finally, the effectiveness of the two proposed control approaches has been validated under random low and high level disturbances as compared with a benchmark controller. The simulation results showed the effectiveness of the first proposal at low level disturbances, as well as proved the robustness of the second proposed control approach at low and high level disturbances.

6.2 Future Work

Future work in the field of MGs may include:

1- Extending the proposed control approaches to be applicable for autonomous microgrids.

2- Inclusion of other types of DGs in the MG Model, such as wind, fuel cells, and hydropower generators.

3- Modeling the MG system based on real data of an existing MG project.

4- Implementation of other energy storage technologies such as super-capacitor energy storage systems and superconducting magnetic energy storage systems.

5- Investigations of the possibility of implementing hybrid energy storage systems with different acting time responses.

6- Testing and validating the proposed control approaches in Real-Time Digital Simulator (RTDS).

7- Exploring other kinds of optimization, such as Biogeography-based optimization technique and machine learning.

8- Exploring other kinds of artificial intelligence techniques such as and machine learning.

References

[1] T. S. Ustun, C. Ozansoy, and A. Zayegh, "Recent Developments in Microgrids and Example Cases Around The World—A Review," *Renewable Sustainable Energy Reviews*, vol. 15, no. 8, pp. 4030-4041, 2011.

[2] N. Lidula and A. Rajapakse, "Microgrids Research: A Review of Experimental Microgrids and Test Systems," *Renewable Sustainable Energy Reviews*, vol. 15, no. 1, pp. 186-202, 2011.

[3] Naderi, Y., Hosseini, S. H., Zadeh, S. G., Mohammadi-Ivatloo, B., Vasquez, J. C., and Guerrero, J. M. "An Overview of Power Quality Enhancement Techniques Applied to Distributed Generation in Electrical Distribution Networks", *Renewable and Sustainable Energy Reviews*, pp. 201-214, 93, 2018.

[4] S. M. Kaviri, M. Pahlevani, P. Jain, and A. Bakhshai, "A Review of AC Microgrid Control Methods," in *the 8th International Symposium on Power Electronics for Distributed Generation Systems (PEDG)*, 2017.

[5] M. Khalid, U. Akram, and S. Shafiq, "Optimal Planning of Multiple Distributed Generating Units and Storage in Active Distribution Networks," *IEEE Access*, 2018.

[6] H. Jiayi, J. Chuanwen, and X. Rong, "A Review on Distributed Energy Resources and Microgrid," *Renewable Sustainable Energy Reviews*, vol. 12, no. 9, pp. 2472-2483, 2008.

[7] M. S. Mahmoud, S. A. Hussain, and M. A. Abido, "Modeling and Control of Microgrid: An Overview," *Journal of the Franklin Institute*, vol. 351, no. 5, pp. 2822-2859, 2014.

[8] P. Basak, S. Chowdhury, S. H. nee Dey, and S. Chowdhury, "A Literature Review on Integration of Distributed Energy Resources in the Perspective of Control, Protection and Stability of Microgrid," *Renewable Sustainable Energy Reviews*, vol. 16, no. 8, pp. 5545-5556, 2012.

[9] T. Green and M. Prodanović, "Control of Inverter-Based Micro-Grids," E*lectric Power Systems Research*, vol. 77, no. 9, pp. 1204-1213, 2007.

[10] M. Kumar and B. Tyagi, "A State of Art Review of Microgrid Control and Integration Aspects," in *the 7th India International Conference on Power Electronics (IICPE)*, Patiala, India, 2016.

[11] I. Vechiu, O. Curea, A. Llaria, and H. Camblong, "Control of Power Converters for Microgrids," *COMPEL*, vol. 30, no. 1, pp. 300-309, 2011.

[12] M. N. Marwali, J.-W. Jung, and A. Keyhani, "Control of Distributed Generation Systems-Part II: Load Sharing Control," *IEEE Transactions on Power Electronics*, vol. 19, no. 6, pp. 1551-1561, 2004.

[13] J. M. Carrasco et al., "Power-Electronic Systems for the Grid Integration of Renewable Energy Sources: A Survey," *IEEE Transactions on Industrial Electronics*, vol. 53, no. 4, pp. 1002-1016, 2006.

[14] F. Blaabjerg, Z. Chen, and S. B. Kjaer, "Power Electronics as Efficient Interface in Dispersed Power Generation Systems," *IEEE Transactions on Power Electronics*, vol. 19, no. 5, pp. 1184-1194, 2004.

[15] F. Katiraei, M. R. Iravani, and P. W. Lehn, "Micro-Grid Autonomous Operation During and Subsequent to Islanding Process," *IEEE Transactions on Power Delivery*, vol. 20, no. 1, pp. 248-257, 2005.

[16] A. G. Tsikalakis and N. D. Hatziargyriou, "Centralized Control for Optimizing Microgrids Operation," in *Power and Energy Society General Meeting*, 2011.

[17] R. Zamora and A. Srivastava, "Controls for Microgrids with Storage: Review, Challenges, and Research Needs," *Renewable Sustainable Energy Reviews*, vol. 14, no. 7, pp. 2009-2018, 2010.

[18] P. F. Ribeiro, B. K. Johnson, M. L. Crow, A. Arsoy, and Y. Liu, "Energy Storage Systems for Advanced Power Applications," *Proceedings of the IEEE*, vol. 89, no. 12, pp. 1744-1756, 2001.

[19] U. Akram and M. Khalid, "A Coordinated Frequency Regulation Framework Based on Hybrid Battery-Ultracapacitor Energy Storage Technologies," *IEEE Access*, vol. 6, pp. 7310-7320, 2018.

[20] M. Faisal, M. Hannan, P. J. Ker, A. Hussain, M. Mansur, and F. Blaabjerg, "Review of Energy Storage System Technologies in Microgrid Applications: Issues and Challenges," *IEEE Access*, 2018.

[21] U. Akram, M. Khalid and S. Shafiq, "Optimal sizing of a wind/solar/battery hybrid grid-connected microgrid system," in *IET Renewable Power Generation*, vol. 12, no. 1, pp. 72-80, 8 1 2018.

[21] A. A. Hamad, M. E. Nassar, E. F. El-Saadany and M. M. A. Salama, "Optimal Configuration of Isolated Hybrid AC/DC Microgrids," in *IEEE Transactions on Smart Grid*, vol. 10, no. 3, pp. 2789-2798, May 2019.

[23] J. Alshehri and M. Khalid, "Power Quality Improvement in Microgrids Under Critical Disturbances Using an Intelligent Decoupled Control Strategy Based on Battery Energy Storage System," in *IEEE Access*, vol. 7, pp. 147314-147326, 2019.

[24] A. M. Jadhav, N. R. Patne and J. M. Guerrero, "A Novel Approach to Neighborhood Fair Energy Trading in a Distribution Network of Multiple Microgrid Clusters," in *IEEE Transactions on Industrial Electronics*, vol. 66, no. 2, pp. 1520-1531, Feb. 2019.

[25] F. Ahmad, M. S. Alam and M. Shahidehpour, "Profit Maximization of Microgrid Aggregator Under Power Market Environment," in *IEEE Systems Journal*, vol. 13, no. 3, pp. 3388-3399, Sept. 2019.

[26] B. Zhao, J. Chen, L. Zhang, X. Zhang, R. Qin, and X. Lin, "Three representative Island Microgrids in the East China Sea: Key Technologies and Experiences," *Renewable Sustainable Energy Reviews*, vol. 96, pp. 262-274, 2018.

[27] A. López-González, B. Domenech, and L. Ferrer-Martí, "Sustainability and Design Assessment of Rural Hybrid Microgrids in Venezuela," *Energy*, vol. 159, pp. 229-242, 2018.

[28] Roman-Barri M., Cairo-Molins I., Sumper A., and Sudria-Andreu A. "Experience on the Implementation of a Microgrid Project in Barcelona.", in *the 2010 IEEE PES Innovative Smart Grid Technologies Conference Europe (ISGT Europe)*, 2010.

[29] M. H. Bellido, L. P. Rosa, A. O. Pereira, D. M. Falcão, and S. K. Ribeiro, "Barriers, Challenges and Opportunities for Microgrid Implementation: The Case of Federal University of Rio de Janeiro," *Journal of Cleaner Production*, vol. 188, pp. 203-216, 2018.

[30] W. Feng et al., "A Review of Microgrid Development in the United States–A Decade of Progress on Policies, Demonstrations, Controls, and Software Tools," *Applied Energy*, vol. 228, pp. 1656-1668, 2018.

[31] K. S. A. Sedzro, X. Shi, A. J. Lamadrid and L. F. Zuluaga, "A Heuristic Approach to the Post-Disturbance and Stochastic Pre-Disturbance Microgrid Formation Problem," in *IEEE Transactions on Smart Grid*, vol. 10, no. 5, pp. 5574-5586, Sept. 2019.

[32] C. Wang, J. Li and Y. Hu, "Frequency Control of Isolated Wind-Diesel Microgrid Power System by Double Equivalent-Input-Disturbance Controllers," in *IEEE Access*, vol. 7, pp. 105617-105626, 2019.

[33] M. E. G. Urias, E. N. Sanchez, and L. J. Ricalde, "Electrical Microgrid Optimization via a New Recurrent Neural Network," *IEEE Systems Journal*, vol. 9, no. 3, pp. 945-953, 2015.

[34] G. Pathak, B. Singh and B. K. Panigrahi, "Wind–Hydro Microgrid and Its Control for Rural Energy System," in *IEEE Transactions on Industry Applications*, vol. 55, no. 3, pp. 3037-3045, May-June 2019.

[35] G. Oriti, N. Anglani and A. L. Julian, "Hybrid Energy Storage Control in a Remote Military Microgrid With Improved Supercapacitor Utilization and Sensitivity Analysis," in *IEEE Transactions on Industry Applications*, vol. 55, no. 5, pp. 5099-5108, Sept.-Oct. 2019.

[36] T. Kerdphol, F. S. Rahman, M. Watanabe and Y. Mitani, "Robust Virtual Inertia Control of a Low Inertia Microgrid Considering Frequency Measurement Effects," in *IEEE Access*, vol. 7, pp. 57550-57560, 2019.

[37] S. Kotra and M. K. Mishra, "Design and Stability Analysis of DC Microgrid With Hybrid Energy Storage System," in *IEEE Transactions on Sustainable Energy*, vol. 10, no. 3, pp. 1603-1612, July 2019.

[38] Y. Song, D. J. Hill and T. Liu, "Impact of DG Connection Topology on the Stability of Inverter-Based Microgrids," in *IEEE Transactions on Power Systems*, vol. 34, no. 5, pp. 3970-3972, Sept. 2019.

[39] B. Fan, J. Peng, J. Duan, Q. Yang and W. Liu, "Distributed control of multiple-bus microgrid with paralleled distributed generators," in *IEEE/CAA Journal of Automatica Sinica*, vol. 6, no. 3, pp. 676-684, May 2019.

[40] J. Alshehri, A. Alzahrani and M. Khalid, "Wind Energy Conversion Systems and Artificial Neural Networks: Role and Applications," 2019 *IEEE Innovative Smart Grid Technologies - Asia (ISGT Asia)*, Chengdu, China, pp. 1777-1782, 2019.

[41] G. P. Holdmann, R. W. Wies and J. B. Vandermeer, "Renewable Energy Integration in Alaska's Remote Islanded Microgrids: Economic Drivers, Technical Strategies, Technological Niche Development, and Policy Implications," in *Proceedings of the IEEE*, vol. 107, no. 9, pp. 1820-1837, Sept. 2019.

[42] I. Das and C. A. Cañizares, "Renewable Energy Integration in Diesel-Based Microgrids at the Canadian Arctic," in *Proceedings of the IEEE*, vol. 107, no. 9, pp. 1838-1856, Sept. 2019.

[43] M. A. Abdulgalil, M. Khalid and J. Alshehri, "Microgrid Reliability Evaluation Using Distributed Energy Storage Systems," 2019 *IEEE Innovative Smart Grid Technologies - Asia (ISGT Asia)*, Chengdu, China, pp. 2837-2841, 2019.

[44] Farrokhabadi, M., König, S., Cañizares, C. A., Bhattacharya, K., and Leibfried, T. "Battery Energy Storage System Models for Microgrid Stability Analysis and Dynamic Simulation", *IEEE Transactions on Power Systems*, vol. 33, no. 2, pp. 2301-2312, 2018.

[45] H. Xie, X. Teng, Y. Xu and Y. Wang, "Optimal Energy Storage Sizing for Networked Microgrids Considering Reliability and Resilience," in *IEEE Access*, vol. 7, pp. 86336-86348, 2019.

[46] M. Ruiz-Cortés et al., "Optimal Charge/Discharge Scheduling of Batteries in Microgrids of Prosumers," in *IEEE Transactions on Energy Conversion*, vol. 34, no. 1, pp. 468-477, March 2019.

[47] Y. Han, X. Ning, P. Yang and L. Xu, "Review of Power Sharing, Voltage Restoration and Stabilization Techniques in Hierarchical Controlled DC Microgrids," in *IEEE Access*, vol. 7, pp. 149202-149223, 2019.

[48] F. Nejabatkhah, Y. W. Li and H. Tian, "Power Quality Control of Smart Hybrid AC/DC Microgrids: An Overview," in *IEEE Access*, vol. 7, pp. 52295-52318, 2019.

[49] Olivares E., Ali Mehrizi-Sani, Amir H., Claudio A. C., Reza I., Mehrdad K., Amir H. H. and et al. "Trends in Microgrid Control." *IEEE Transactions on Smart Grid*, vol. 5, no. 4, pp. 1905-1919, 2014.

[50] S. Parhizi, H. Lotfi, A. Khodaei, and S. Bahramirad, "State of the Art in Research on Microgrids: A Review," *IEEE Access*, vol. 3, no. 1, pp. 890-925, 2015.

[51] H. Bevrani, F. Habibi, P. Babahajyani, M. Watanabe, and Y. Mitani, "Intelligent Frequency Control in an AC Microgrid: Online PSO-Based Fuzzy Tuning Approach," *IEEE Transactions on Smart Grid*, vol. 3, no. 4, pp. 1935-1944, 2012.

[52] W. Su and J. Wang, "Energy Management Systems in Microgrid Operations," *Electricity Journal*, vol. 25, no. 8, pp. 45-60, Oct. 2012.

[53] D. E. Olivares, C. A. Canizares, and M. Kazerani, "A Centralized Optimal Energy Management System for Microgrids," in *Proceedings of IEEE Power and Energy Society General Meeting*, Jul. 2011.

[54] M. Prodanovic and T. C. Green, "High-Quality Power Generation through Distributed Control of a Power Park Microgrid," *IEEE Transactions on Industrial Electronics*, vol. 53, no. 5, pp. 1471-1482, Oct. 2006.

[55] N. L. Díaz, A. C. Luna, J. C. Vasquez and J. M. Guerrero, "Centralized Control Architecture for Coordination of Distributed Renewable Generation and Energy Storage in Islanded AC Microgrids," in *IEEE Transactions on Power Electronics*, vol. 32, no. 7, pp. 5202-5213, July 2017.

[56] K. Rajesh, S. Dash, R. Rajagopal, and R. Sridhar, "A Review on Control of AC Microgrid," *Renewable Sustainable Energy Reviews*, vol. 71, pp. 814-819, 2017.

[57] Z. Zhang, C. Dou, D. Yue, B. Zhang, and W. Luo, "A Decentralized Control Method for Frequency Restoration and Accurate Reactive Power Sharing in Islanded Microgrids," *Journal of the Franklin Institute*, 2018.

[58] P. Yang, Y. Xia, M. Yu, W. Wei, and Y. Peng, "A Decentralized Coordination Control Method for Parallel Bidirectional Power Converters in a Hybrid AC–DC Microgrid," *IEEE Transactions on Industrial Electronics*, vol. 65, no. 8, pp. 6217-6228, 2018.

[59] H. Liang, B. J. Choi,W. Zhuang, and X. Shen, "Stability Enhancement of Decentralized Inverter Control through Wireless Communications in Microgrids," *IEEE Transactions on Smart Grid*, vol. 4, no. 1, pp. 321-331, Mar. 2013.

[60] J. Kim, J. M. Guerrero, P. Rodriguez, R. Teodorescu, and K. Nam, "Mode Adaptive Droop Control with Virtual Output Impedances for an Inverter-Based Flexible AC Microgrid," *IEEE Transactions on Power Electronics*, vol. 26, no. 3, pp. 689-701, Mar. 2011.

[61] J. Shah, B. F. Wollenberg, and N. Mohan, “Decentralized Power Flow Control for a Smart Micro-Grid," in t*he Proceedings of the IEEE Power Energy Society General Meeting*, Jul. 2011.

[62] Wu, D., Tang, F., Dragicevic, T., Vasquez, J. C., and Guerrero, J. "A Control Architecture to Coordinate Renewable Energy Sources and Energy Storage Systems in Islanded Microgrids." *IEEE Transactions on Smart Grid*, pp. 1156-1166, 2014.

[63] A. R. Khatib, B. Nayak, B. Dai, J. Coleman, S. Hoskins, and J. Tierson, "Design and Development of a Microgrid Control System for Integration of Induction Generation with Storage Capability at Saint Paul Island, Alaska," in *the IEEE Innovative Smart Grid Technologies Conference (ISGT)*, 2017.

[64] M. Saleh, Y. Esa, and A. Mohamed, "Centralized Control for DC Microgrid Using Finite State Machine," in *the IEEE Innovative Smart Grid Technologies Conference (ISGT)*, 2017.

[65] X. Huang, K. Wang, J. Qiu, L. Hang, G. Li and X. Wang, "Decentralized Control of Multi-Parallel Grid-Forming DGs in Islanded Microgrids for Enhanced Transient Performance," in *IEEE Access*, vol. 7, pp. 17958-17968, 2019.

[66] L. Li, Y. Sun, Z. Liu, X. Hou, G. Shi and M. Su, "A Decentralized Control With Unique Equilibrium Point for Cascaded-Type Microgrid," in *IEEE Transactions on Sustainable Energy*, vol. 10, no. 1, pp. 324-326, Jan. 2019.

[67] A. Bani-Ahmed, M. Rashidi, A. Nasiri and H. Hosseini, "Reliability Analysis of a Decentralized Microgrid Control Architecture," in *IEEE Transactions on Smart Grid*, vol. 10, no. 4, pp. 3910-3918, July 2019.

[68] J. Peng, B. Fan, J. Duan, Q. Yang and W. Liu, "Adaptive Decentralized Output-Constrained Control of Single-Bus DC Microgrids," in *IEEE/CAA Journal of Automatica Sinica*, vol. 6, no. 2, pp. 424-432, March 2019.

[69] K. Mahmud, A. K. Sahoo, J. Ravishankar and Z. Y. Dong, "Coordinated Multilayer Control for Energy Management of Grid-Connected AC Microgrids," in *IEEE Transactions on Industry Applications*, vol. 55, no. 6, pp. 7071-7081, Nov.-Dec. 2019.

[70] J. Lee, Y. Kim and S. Moon, "Novel Supervisory Control Method for Islanded Droop-Based AC/DC Microgrids," in *IEEE Transactions on Power Systems*, vol. 34, no. 3, pp. 2140-2151, May 2019.

[71] C. Wang, J. Duan, B. Fan, Q. Yang and W. Liu, "Decentralized High-Performance Control of DC Microgrids," in *IEEE Transactions on Smart Grid*, vol. 10, no. 3, pp. 3355-3363, May 2019.

[72] H. Mahmood and J. Jiang, "Decentralized Power Management of Multiple PV, Battery, and Droop Units in an Islanded Microgrid," in *IEEE Transactions on Smart Grid*, vol. 10, no. 2, pp. 1898-1906, March 2019.

[73] R. Al Badwawi, W. R. Issa, T. K. Mallick and M. Abusara, "Supervisory Control for Power Management of an Islanded AC Microgrid Using a Frequency Signalling-Based Fuzzy Logic Controller," in *IEEE Transactions on Sustainable Energy*, vol. 10, no. 1, pp. 94-104, Jan. 2019.

[74] U. Akram, M. Khalid, and S. Shafiq, "An Innovative Hybrid Wind-Solar and Battery-Supercapacitor Microgrid System—Development and Optimization," *IEEE Access*, vol. 5, pp. 25897-25912, 2017.

[75] J. Choi, Y. Shin, M. Choi, W. Park and I. Lee, "Robust Control of a Microgrid Energy Storage System Using Various Approaches," in *IEEE Transactions on Smart Grid*, vol. 10, no. 3, pp. 2702-2712, May 2019.

[76] Toma, Lucian, et al. "On the Virtual Inertia Provision by BESS in Low Inertia Power Systems." In *the 2018 IEEE International Energy Conference (ENERGYCON)*, 2018.

[77] Serban, I., and C. Marinescu. "Battery Energy Storage System for Frequency Support in Microgrids and with Enhanced Control Features for Uninterruptible Supply of Local Loads." *International Journal of Electrical Power & Energy Systems*, pp. 432-441, 54, 2014.

[78] Delille, G., Bruno F., and Gilles M. "Dynamic Frequency Control Support by Energy Storage to Reduce the Impact of Wind and Solar Generation on Isolated Power System's Inertia", *IEEE Transactions on Sustainable Energy*, vol. 3, no. 4, pp. 931-939, 2012.

[79] Wu D., Tang F., Dragicevic T., Vasquez J. C., and Guerrero J. M. "Autonomous Active Power Control for Islanded AC Microgrids with Photovoltaic Generation and Energy Storage System", *IEEE Transactions on Energy Conversion*, vol. 29, no. 4, pp. 882-892, 2014.

[80] D. I. Brandao, T. Caldognetto, F. P. Marafão, M. G. Simões, J. A. Pomilio and P. Tenti, "Centralized Control of Distributed Single-Phase Inverters Arbitrarily

Connected to Three-Phase Four-Wire Microgrids," in *IEEE Transactions on Smart Grid*, vol. 8, no. 1, pp. 437-446, Jan. 2017.

[81] F. Shahnia, R. Majumder, A. Ghosh, G. Ledwich, and F. Zare, "Operation and Control of a Hybrid Microgrid Containing Unbalanced and Nonlinear Loads," *Electric Power System. Research*, vol. 80, no. 8, pp. 954-965, Aug. 2010.

[82] Adrian Timbus, Marco Liserre, Remus Teodorescu, Pedro Rodriguez, and Frede Blaabjerg, "Evaluation of Current Controllers for Distributed Power Generation Systems", *IEEE Transactions on Power Electronics*, Vol. 24, No. 3, pp. 654-664, 2009.

[83] W. Feng, K. Sun, Y. Guan, J. M. Guerrero and X. Xiao, "Active Power Quality Improvement Strategy for Grid-Connected Microgrid Based on Hierarchical Control," in *IEEE Transactions on Smart Grid*, vol. 9, no. 4, pp. 3486-3495, July 2018.

[84] G. Parise, L. Martirano, M. Kermani, and M. Kermani, "Designing a Power Control Strategy in a Microgrid Using PID/Fuzzy Controller Based on Battery Energy Storage," in t*he International Conference on Environment and Electrical Engineering (EEEIC)*, Milan, Italy, 2017.

[85] M. Kermani, "Transient Voltage and Frequency Stability of an Isolated Microgrid Based on Energy Storage Systems," in *the International Conference on Environment and Electrical Engineering (EEEIC)*, Florence, Italy, 2016.

[86] J. Alshehri, M. Khalid, and A. Alzahrani, "An Intelligent Battery Energy Storage-Based Controller for Power Quality Improvement in Microgrids," *Energies*, vol. 12, no. 11, p. 2112, 2019.

[87] H. Li, X. Wang, and J. Xiao, "Differential Evolution-Based Load Frequency Robust Control for Micro-Grids with Energy Storage Systems," *Energies*, vol. 11, no. 7, p. 1686, 2018.

[88] M. A. Ali, "Control of a Microgrid Through Energy Storage Devices Using Evolutionary and Neuro-Fuzzy Methods," *Master Thesis*, King Fahd University of Petroleum and Minerals Dhahran, Saudi Arabia, 2013.

[89] C. Fu and W. Tan, "Decentralised Load Frequency Control for Power Systems with Communication Delays via Active Disturbance Rejection," *IET Generation, Transmission & Distribution*, vol. 12, no. 6, pp. 1397-1403, 2017.

[90] M. Ma, C. Zhang, X. Liu, and H. Chen, "Distributed Model Predictive Load Frequency Control of the Multi-Area Power System After Deregulation," *IEEE Transactions on Industrial Electronics*, vol. 64, no. 6, pp. 5129-5139, 2017.

[91] R. Shankar, K. Chatterjee, and R. Bhushan, "Impact of Energy Storage System on Load Frequency Control for Diverse Sources of Interconnected Power System in Deregulated Power Environment," *International Journal of Electrical Power Energy Systems*, vol. 79, pp. 11-26, 2016.

[92] C. Mu, Y. Tang, and H. He, "Improved Sliding Mode Design for Load Frequency Control of Power System Integrated an Adaptive Learning Strategy," *IEEE Transactions on Industrial Electronics*, vol. 64, no. 8, pp. 6742-6751, 2017.

[93] G. Rinaldi, M. Cucuzzella, and A. Ferrara, "Third Order Sliding Mode Observer-Based Approach for Distributed Optimal Load Frequency Control," *IEEE Control Systems Letters*, vol. 1, no. 2, pp. 215-220, 2017.

[94] H. Yan, X. Zhou, H. Zhang, F. Yang and Z. Wu, "A Novel Sliding Mode Estimation for Microgrid Control With Communication Time Delays," in *IEEE Transactions on Smart Grid*, vol. 10, no. 2, pp. 1509-1520, March 2019.

[95] N. M. Dehkordi, H. R. Baghaee, N. Sadati and J. M. Guerrero, "Distributed Noise-Resilient Secondary Voltage and Frequency Control for Islanded Microgrids," in *IEEE Transactions on Smart Grid*, vol. 10, no. 4, pp. 3780-3790, July 2019.

[96] H. Zhao, M. Hong, W. Lin and K. A. Loparo, "Voltage and Frequency Regulation of Microgrid With Battery Energy Storage Systems," in *IEEE Transactions on Smart Grid*, vol. 10, no. 1, pp. 414-424, Jan. 2019.

[97] K. W. Joung, T. Kim and J. Park, "Decoupled Frequency and Voltage Control for Stand-Alone Microgrid With High Renewable Penetration," in *IEEE Transactions on Industry Applications*, vol. 55, no. 1, pp. 122-133, Jan.-Feb. 2019.

[98] M. Zhang et al., "Cooperative Operation of DG Inverters and a RIHAF for Power Quality Improvement in an Integrated Transformer-Structured Grid-Connected Microgrid," in *IEEE Transactions on Industry Applications*, vol. 55, no. 2, pp. 1157-1170, March-April 2019.

[99] M. A. Shoeb, F. Shahnia and G. M. Shafiullah, "A Multilayer and Event-Triggered Voltage and Frequency Management Technique for Microgrid’s Central Controller Considering Operational and Sustainability Aspects," in *IEEE Transactions on Smart Grid*, vol. 10, no. 5, pp. 5136-5151, Sept. 2019.

[100] D. Dasgupta and Z. Michalewicz, Evolutionary Algorithms in Engineering Applications, *Springer Science & Business Media*, 2013.

[101] R. Storn, "On the Usage of Differential Evolution for Function Optimization," in *Biennial Conference of the North American Fuzzy Information Processing Society (NAFIPS)*, Berkeley, California, USA, 1996.

[102] K. J. Åström and T. Hägglund, "Revisiting the Ziegler–Nichols Step Response Method for PID Control," *Journal of Process Control*, vol. 14, no. 6, pp. 635-650, 2004.

[103] S. Das and P. N. Suganthan, "Differential Evolution: A Survey of the State-of-the-art," *IEEE Transactions on Evolutionary Computation*, vol. 15, no. 1, pp. 4-31, 2010.

[104] M. T. Hagan and M. B. Menhaj, "Training Feedforward Networks with the Marquardt Algorithm," *IEEE Transactions on Neural Networks*, vol. 5, no. 6, pp. 989-993, 1994.

[105] B. Mohanty, S. Panda, and P. Hota, "Controller Parameters Tuning of Differential Evolution Algorithm and its Application to Load Frequency Control of Multi-Source Power System," *International Journal of Electrical Power & Energy Systems*, vol. 54, pp. 77-85, 2014.

Vitae

Name	: Jaber Ali Alshehri
Nationality	: Saudi
Date of Birth	: 10/17/1992
Email	: jaber.a.shehri@gmail.com
Address	: Dammam, Saudi Arabia
Academic Background	: **MSc of Electrical Engineering (Power)**
	December, 2019.
	King Fahd University of Petroleum and Minerals,
	Dhahran, Saudi Arabia.
	BSc of Electrical Engineering
	January, 2016.
	King Fahd University of Petroleum and Minerals,
	Dhahran, Saudi Arabia.